Norwegian University of Life Sciences

Master's Thesis 2023 60 ECTS
Faculty of Biosciences

Yield prediction in ryegrass with UAV-based RGB and multispectral imaging

Hedda Charlotte Haugland
M Sc. Plant science

Acknowledgement

I would like to express my gratitude to my supervisor Sahameh Shafiee, for all her time, guidance, patience, suggestions, and UAV training. More than anything else, I appreciate the academic freedom and the tremendous support I received.

I am very grateful for my co-supervisors Marian Schubert and Helga Amdahl for their professional advice, training, ideas, and instruction for the fieldwork, and the comments to improve the manuscript. It would not be possible for me to finish my work without their encouragement and constructive criticism.

I am also very grateful for the HighGrass project and want to thank so much for the possibility to pursue and learn so much about this exciting subject area and giving me the possibility to extend my knowledge further in plant breeding of forage grasses and precision technology.

Special thanks to Henrik Lassegård and Tomasz Mroz for all the help with the UAVs and for answering my questions for both UAV technically and the data processing and programming and all the helpful tips and demonstration for how I could solve it my selves.

I'm also grateful for my study friends supporting me and reminding me to take some breaks. A special thanks to my good friend Guro Herborg Ørmen Bukaasen for all hours companying me in the field while flying, and for all the moral support.

Lastly, I would be remiss in not mentioning my family and friends. Their belief in me has kept my spirits and motivation high during this whole process. I would also like to thank my dog for all the entertainment and emotional support.

Abstract

Forage grass breeding is time-consuming and costly, with the need for special knowledge and experience to make the right decisions for future forage grass production. All measurements for decision-making require manual labor and hands-on inspections. For the yield trait, the traditional method of measurement is cutting and weighing the grass. New methods for yield prediction and measurement with Unmanned Aerial Vehicle (UAV) have been tested on different crops with good results. For perennial ryegrass *(Lolium perenne L.)* yield prediction has earlier been performed on plots with a flight altitude for image capturing at 20 meters and which has yielded promising results for our study.

This study has been exploring different flight altitudes for ryegrass yield prediction using UAV imagery. The sensors that have been used in this study are multispectral and RGB cameras integrated in the UAVs. Our study consists of two trials with pre-selected varieties of perennial ryegrass, one with diploid varieties and one with tetraploid varieties and mixtures between diploid and tetraploid varieties, were investigated. Both trials were seeded at two different locations in Norway. Varieties were planted as rows for the first location (Vollebekk, Ås, Norway) while for the second location (Arneberg, Ilseng, Norway) the two trials were planted as both rows and plots. The dry matter yield (DMY) data were collected with traditional harvest four times for the rows, and three times for the plots. The UAV-images were collected at different flight altitudes with both multispectral and RGB cameras. The full data processing routine was conducted on the first and second cut for both locations. Multivariate regression model was applied for DMY prediction based on UAV imagery.

The results correlated well with the predictions at Ås for both multispectral images as well as RGB methods of image acquisition. Our results indicated a high correlation between the actual DMY and the predicted DMY from both RGB images as well as multispectral images with a correlation coefficient on 0.92 for both, but at different assessment dates. The maximum correlation was acquired for the first cut from location Ås.

For location Arneberg, the acquired images could not yield results of sufficient quality, and thus, no predictions could be made.

Sammendrag

Engvekst foredling er både tidskrevende og dyrt. Det kreves et behov for kunnskap og erfaring for å ta gode og riktige vurderinger, samt beslutninger for å dekke det kommende behovet fôrproduksjonen vil møte i framtiden. Alle målingene og vurderingene som ligger til grunn for riktige beslutninger krever en del manuelt arbeid og nærmere inspeksjon av plantene. For egenskapen som går på avling, blir disse målt med tradisjonell slått, og videre tørket for tørrstoff-prosent. Nye metoder for avlingsprediksjon og målinger gjort med droner har blitt utprøvd i flere planteproduksjoner med gode resultater. For flerårig raigras *(Lolium perenne L.)* har avlingsprediksjon blitt gjennomført på ruter, med dronebilder fra 20 meters høyde, og gitt lovende resultater for vårt forsøk.

I dette forsøket har det blitt testet ut fire ulike høyder for flyving med drone for fotografering og avlingsprediksjon av raigras-feltene. Det har blitt brukt to ulike droner i dette forsøket, begge har vært droner med monterte kameraer. Den ene har vært montert med et multispektralt kamera, mens den andre har vært montert med et standard RGB kamera. Det ble anlagt to felter med forhåndsutvalgte populasjoner og sorter av raigras, en med diploide sorter, og en med tetraploide sorter og blandinger mellom en diploid og en eller flere tetraploide sorter. Begge feltene har blitt sådd på to forskjellige steder i Norge. Den første lokasjonen ble sådd som rader på Vollebekk (Ås, Norge). På den andre lokasjonen ble sådd som både rader og ruter på Arneberg (Ilseng, Norge). De fenotypiske dataene ble innsamlet gjennom tradisjonell slått med slåmaskin og tørking for tørrstoffinnholdet. Dette ble gjennomført fire ganger for radene, og tre ganger for rutene. Dronefotograferingen ble gjennomført ved å følge en forhåndsutviklet tidsplan med spesifikke tider, høyder og kameraspesifikasjoner. Komplett dataprosessering med avlingsprediksjon ble gjennomført for første og andre slått på begge lokasjoner. En multivariat regresjonsmodell ble brukt for DMY prediksjon med UAV-bildene.

Resultatene våre fra Ås lokasjonen korrelerte godt med avling, og den høyeste korrelasjons koeffisienten som ble oppnådd på avlingspredikasjon var basert på multispektrale og RGB bilder fra Ås lokasjonen og DMY fra første slått. Avlingspredikasjonen basert på både multispektrale bilder og RGB bilder ga en korrelasjon koeffisient på 0.92, men fra forskjellige tidspunkt. De innhentede bildene fra Arneberg ga ikke resultater av tilstrekkelig kvalitet, så derfor kunne ikke predikasjon gjennomføres.

Abbreviations

UAV- Unmanned aerial vehicle

RGB- Red, Green, and Blue

NDVI- Normalized Difference Vegetation Index (NIR-R/NIR+R)

NIR- Near-Infrared

DMY- Dry matter yield

GCP- Ground control point

GCI- Green Chlorophyll Index (NIR/Green)-1

Tetraploid- four sets of chromosomes.

Diploid- two sets of chromosomes.

DSS- Decision Support system

FW – Fresh weight

VI – Vegetation Indices

DSM – Digital Surface Model (https://support.pix4d.com/hc/en-us/articles/360048706771-DSM-PIX4Dmatic)

DTM – Digital terrain Model (https://support.pix4d.com/hc/en-us/articles/202560579-How-to-automatically-generate-a-Digital-Terrain-Model-DTM)

Table of Contents

1. Introduction

1.1 Background

1.1.1 Perennial ryegrass

Lolium perenne L. is one of the most researched and valuable temperate pasture grasses in the world (Cunningham et al., 1994). Perennial ryegrass is also a widely used forage grass among farmers in dairy and sheep production and has become the most sown perennial grass in temperate regions due to its high tolerance for grazing(Wilkins & Humphreys, 2003). For the farmer, the fast establishment and high yield potential is essential for efficient and economical production (Jung et al., 1996). For the animal production, desirable traits such as the taste and high digestibility of ryegrass highly favored by the animals is crucial (Frame, 1989). Ryegrass is also very suitable for reduced-tillage renovation and use for heavy and waterlogged soil (Hannaway et al., 1999). These traits are advantageous with regards to an upcoming popularity in farming with reduced tillage for carbon-saving.

1.1.2 Forage grass production

In Norway, only 3,5% of land area is used for farming (Fakta om Landbruk, 2023), and due to the topography and climate conditions, only 1/3 of farmlands equivalent to 1% of total landmass is used for food production directly for humans, such as cereals, vegetables, legumes, and oil crops. Forage grass production is the biggest production in Norway, with almost 2/3 of all farmland used for this purpose (Steinshamn et al., 2016). Most pastures and forage grass fields are sown with seed mixture, a combination with several different species to make an optimal canopy composition for a high-quality and high-yield harvest, as well as hardy and strong fields that can withstand winter conditions and normal exposure to heavy machinery, and still produce yield for many years. The forage production in Norway mostly includes ryegrass as a part of a seed mixtures. A commonly used seed mixture include timothy (Phleum pratense), red and white clover (Trifolium pratense), perennial ryegrass, meadow fescue (Festuca pratensis), and smooth meadow-grass (Poa pratensis) (Repstad, 2023).

1.1.3 Forage grass breeding

Increasing biomass production in forage grasses by increasing the annual and seasonal dry matter yield (DMY) while also improving the frost and drought tolerance, persistence, disease resistance and yield quality is the main goal for breeders (Pranga et al., 2021). Biomass yield is a very complex trait. It is impacted by the variations in tillering, growth habits of the plant, the duration of the season (heat sum), growth environments, plant age, and regrowth after defoliation. (Gebremedhin et al., 2020; Yates et al., 2019)

The early stages of perennial ryegrass breeding programs usually depend on the assessment of populations based on large number of genotypes planted as spaced plants or small plots in the field (Gebremedhin et al., 2020; Ghamkhar et al., 2019; Lootens et al., 2016). These types of assessments involves many different measurements and selection procedures across seasons and years to evaluate biomass yield repeatedly (Leddin et al., 2018). To accommodate the plant breeders and their need to collect a large amount of accurate yield data both rapidly and cost efficient, a protocol for yield prediction with the use of UAV-imagery could be advantageous (Bhandari et al., 2023). Since the forage grass breeders base their selections on visual scores of genotypes and populations, scoring thousands of plants or plots is time-intensive and laborious task. With UAV-imaging it can take down to a matter of minutes to fly over the site and capture the image data (Wang et al., 2019).

1.1.4 Phenotyping tools

Well-developed phenotyping tools such as sensors for measurement and monitoring are essential for precision agriculture and new development in plant breeding. Phenotyping, being the cornerstone in plant breeding (Reynolds et al., 2020), is still the bottleneck for the development of techniques for a more precise and accurate recording of important agronomical traits (Alckmin et al., 2022; Araus & Cairns, 2014; Burud et al., 2017; Rallo et al., 2020; Song et al., 2021). Reliable tools for imaging and sensing need to be developed and tested in order to allow for a precise phenotyping. The monumental challenge of precision agriculture lays in the identification of cheap, robust, easy-to-use, rapid and automated phenotyping methods. To properly make use of UAVs, the protocol needs to be so precise that the predictions can be used instead of an actual

harvest in a breeding program where the yield can be measured and predicted with UAV-imaging and the field can be cut without the need of taking samples. Yield prediction with UAV-images has successfully been proven by other studies (Borra-Serrano et al., 2019; Gebremedhin, Badenhorst, Wang, Giri, et al., 2019; Pranga et al., 2021; Shorten & Trolove, 2022).

1.1.5 Unmanned Aerial Vehicles in plant breeding

UAV-imagery is a non-destructive data-collecting method, and the data can be stored and used several times without reducing the quality of the data. (Gebremedhin, Badenhorst, Wang, Spangenberg, et al., 2019). Unmanned Aerial Vehicles (UAV) equipped with RGB, multispectral, hyperspectral, or thermic cameras are proven to be efficient in phenotyping and convenient for the breeder when taking decisions in plant breeding for several productions, such as corn (Barzin et al., 2020), soybeans (Moeinizade et al., 2022), citrus (Ampatzidis & Partel, 2019) and olives (Rallo et al., 2020). Both RGB and multispectral imaging have been found to be more efficient for yield prediction than traditional methods (Xie & Yang, 2020). Traditional methods for measurements relay on rapid inspection in the field taking notes and scoring traits using a scale to state the difference between the plants. UAV-imaging has the ability to detect more features than the human eye. UAV imaging combined with computers and machine-learning, allows for breeders and scientist to inspect and observe changes in the filed, such as drought, ahead of time, or in this case yield before breeders can assess the same results with conventional methods (Ludovisi et al., 2017). For yield prediction with UAV, previous studies have used heights such as 100 meters (Fan et al., 2018), 40 meters and 30 meters (Pranga et al., 2021), 35 meters (Alckmin et al., 2022) and 20 meters (Wang et al., 2019). Shorten & Trolove did a study on ryegrass prediction for DMY with UAV-images from plots (size:1.5- 2.4 m^2), and their findings resulted in a coefficient of determination on 0.61-0.66. (Shorten & Trolove, 2022). Yield prediciton using UAVs has shown promising results for other crops, for example in West Africa, an R^2=0.95 and MAE=0.160 kg/ha has been reported for crops such as cassava and bananas (Cedric et al., 2022). The new UAV-technology can assist the plant breeders in the process of decision-making.

1.1.6 The need for new technology

To accommodate the food productions, and the increased need for food while the world population continues to rise, the farmers need forage grasses that are better suited for the changing climate and potentially more extreme weather so that less yield is lost due to crises such as drought or flood. The plant breeders need to breed the forage grass suited for the upcoming climate almost 30 years in advance.

One way that UAVs and imaging can increase the efficiency of the breeding process is with precise yield predictions, so that the fields don't need to be harvested each time and the grass can just be cut to start the growing process again for the next harvest. This will save the time used for harvesting and sampling. UAV-images can also save the breeder time if the images can be used for inspecting and determine different traits. Then the UAV can be operated by a pilot, and the breeder can use the same time one something else and look at the images later.

Another way UAV imagery, yield prediction and field setup can save space and time in the forage grass breeding programs are with the use of rows instead of plots. This could potentially save field space and make room for more populations to test. For this to happen the results from images taken of rows have to produce the same results as images taken of plots.

1.2Objectives

This study was conducted with the main objective of developing phenotyping tools for Norwegian ryegrass breeding while the following sub-objectives were followed:

- Develop protocols for ryegrass phenotyping using UAV imagery.
- Determine the optimal flight altitude for ryegrass yield prediction and volume measurement.
- DMY prediction using spectral reflectance from five different spectral bands including red, green, blue, reg edge, and NIR.
- Compare the RGB and multispectral imaging capabilities for DMY prediction.

2. Materials and Methods

The method for this experiment is divided in three parts. The first is plant material and collection schedule. This part contains perennial ryegrass breeding lines and field setup. as well as the data collection schedule with the UAV protocol and the different traits to register.

The second part is data assessment, which is the actual data collection. Both phenotypic data and image data has been collected throughout the season with manual inspections, yield harvest and image capturing with both multispectral and RGB camera.

The last step is the data processing, from import and calibration of raw images, to stitching, geo-locating, export, extraction and visualisation and analysis.

Each step is described further in the materials and methods.

2.1 Plant material and experimental design

Perennial ryegrass populations used in this study were divided in two groups. The first group consisted of diploid populations that were chosen based on contrasting phenotypic values of different traits such as, hight (low and high), heading time (early and late), autumn size (big and small), spring growth (slow and fast), growth habit (erect and prostrate), regrowth (slow and fast), rust resistance and winter survival. The second group consisted of available tetraploid varieties and mixtures between tetraploid and diploid varieties. These two groups of populations were tested in two separate trials, diploid trial with 23 populations and tetraploid trial with 20 populations. Trials were established at two locations, at Ås (59°39'43.8"N, 10°44'58.5"E, 85 m.a.s) and at Arneberg (60°45'28.0"N 11°11'41.0"E, 208,5 m.a.s).

The two trials at Ås, were established in rows that were 2 m long (Figure 1.). The two trials at Arneberg were established also in rows that were 2 m long and additionally as plots with size of 6 m^2 (Figure 2). Both trials, rows, and plots, were designed as complete randomized block design with three replications. All trials were established in 2021 while the phenotyping with drones was done in 2022.

Figure 1. Row trials at Ås. Diploid trial with red frame and tetraploid trial with blue frame.

Figure 2. Plot trials (left side) and row trials (right side) at Arneberg. Trials with diploid populations are in red frame and trials with tetraploid populations are in blue frame.

2.2 Data assessment

2.2.1 Assessing yield data by Haldrup harvester

All the row trials were harvested four times throughout the season while the plot trial at Arneberg was harvested three times. Harvesting dates are presented in Table 1.

Table 1. Harvest dates for location Ås and Arneberg

	1.	2.	3.	4.
	First cut	Second cut	Third cut	Fourth cut
Ås	2022-06-02	2022-07-06	2022-08-17	2022-09-20
Arneberg	2022-06-13	2022-07-13	2022-08-07	2022-09-29

Both plots and rows for the data of fresh matter yield were harvested using Haldrup harvester (Figure 19. in Appendix 3.). To measure the rows dry matter yield at Ås, harvested fresh matter yield was dried at 60 degrees Celsius for 2 days weighted again for the accurate dry matter yield (DMY). Dry matter yield of rows and plots at Arneberg were determined by NIR instrument on the harvester.

2.2.2 Assessing yield data using Unmanned Aerial Vehicle (UAV)

Aerial images were captured between 11 a.m. and 2 p.m. by using an unmanned aerial vehicle (UAV, Phantom 4) with both a high-resolution RGB camera and a multispectral camera. The UAV was set to fly automatically according to a set flight plan by the application, DJI GO 4. The two cameras were set to automatically take pictures every two seconds, flown with a speed of approximately 1-2 m/s, and at different altitudes (Table 2). RGB camera captured images with longitudinal and lateral overlaps of 85 and 80 %, respectively, and it flew both perpendicular and horizontal to sowing rows to maximize reconstruction efficiency. The multispectral camera flew with longitudinal and lateral overlaps of 85 and 75%, respectively and it collected images in 5 different bands: red, green, blue, NIR, and Red-Edge. A total of 101 missions were conducted

throughout the season with both cameras. Ground control points (GCPs) were laid out in the fields, four in the corners and one in the middle of the fields, and the coordinates of GCPs were measured using a GPS system. The use of ground control points allows the alignment of orthoimages obtained from different dates by the generation of a georeferenced orthomosaic image. A Calibrated Reflectance Panel (CRP) was also used to calibrate the images for the daily light levels. The CRP was added by including a picture from each of the bands of the multispectral camera from the CRP just before each flight.

Table 2. Flight schedule for all trials at Ås and Arneberg.

Trait	Time	Altitude (m)	Coverage	Drone used
DMY	Once a week during season	20,30,50	85% forward, 75% side	Phantom 4 Multispectral
Regrowth	4,8,12 and16 days after harvest	15,20,30	85% forward, 75% side	Phantom 4 Multispectral Phantom 4 RGB

At Arneberg only two flight heights,15 meters and 20 meters were used. This decision was done early on in the season, so for this location, there is no images for the different cuts at 30 meters and 50 meters.

2.3 Data Processing

Processing of UAV images including geometric correction, image mosaicking, and radiometric calibration was conducted in Pix4D software. (Pix4D SA, Lausanne, Switzerland) as explained in

previous studies (Dobbels & Lorenz, 2019; Khan et al., 2018). For multispectral images, the orthomosaic was generated for each band separately. Geo-referencing was done by pairing the imported ground control points (GCPs) and the GCPs in the images.

QGIS software (QGIS 3.4, Open Source Geospatial Foundation Project. http://qgis.osgeo.org) was used to extract spectral values from each plot in the field. All generated orthomosaics by Pix4D were imported to QGIS 3.28 (Quantum GIS Development Team 2017) to extract the average reflectance or plant height. Five bands including blue, green, red, red edge and NIR were stacked together in QGIS. A vector was created to generate a mask including a polygon for each plot or row in the orthomosaic. Since our focus is on the performance of the whole field trial plots with well-structured canopies, the mixed pixel issue is not considerable in this study. Plot values for each band were calculated as the mean value of the pixels in each plot, where the outer edges were removed to avoid plot border effects.

The zonal statistics function under the raster toolbox was applied to extract values for each polygon and the results were exported as and excel file and saved. Figure 3 sixth step illustrates the extraction of the index values from each row. The polygons are individually made for each row based on their size from an early date, and the same masks are used for every extraction to make the source of error the same, and image of the extraction polygons are pictured in the figure 4 sixth step.

In this study, the 3D models of the digital terrain model (DTM) and the DSM (digital surface model) were created by Pix4D for calculating plant height. The DTM was defined as a model of the underlying field topography without crop features, which is corresponding to the state of no crop growing on the ground, and the DSM was defined as a combined model of the underlying topography and field features such as crops, corresponding to the state of the crop grown (Kim et al., 2018). The DTM was acquired on the first UAV flight when the crops were not germinated on the ground within 7 days after sowing and the DSMs were acquired on each of the USV flight dates. Finally, the plant height, defined as a model of field features only, was calculated by subtracting the DSM from the DTM: Plant Height = DSM-DTM

Figure 3. shows the workflow for the data processing in Pix4D and Qgis.

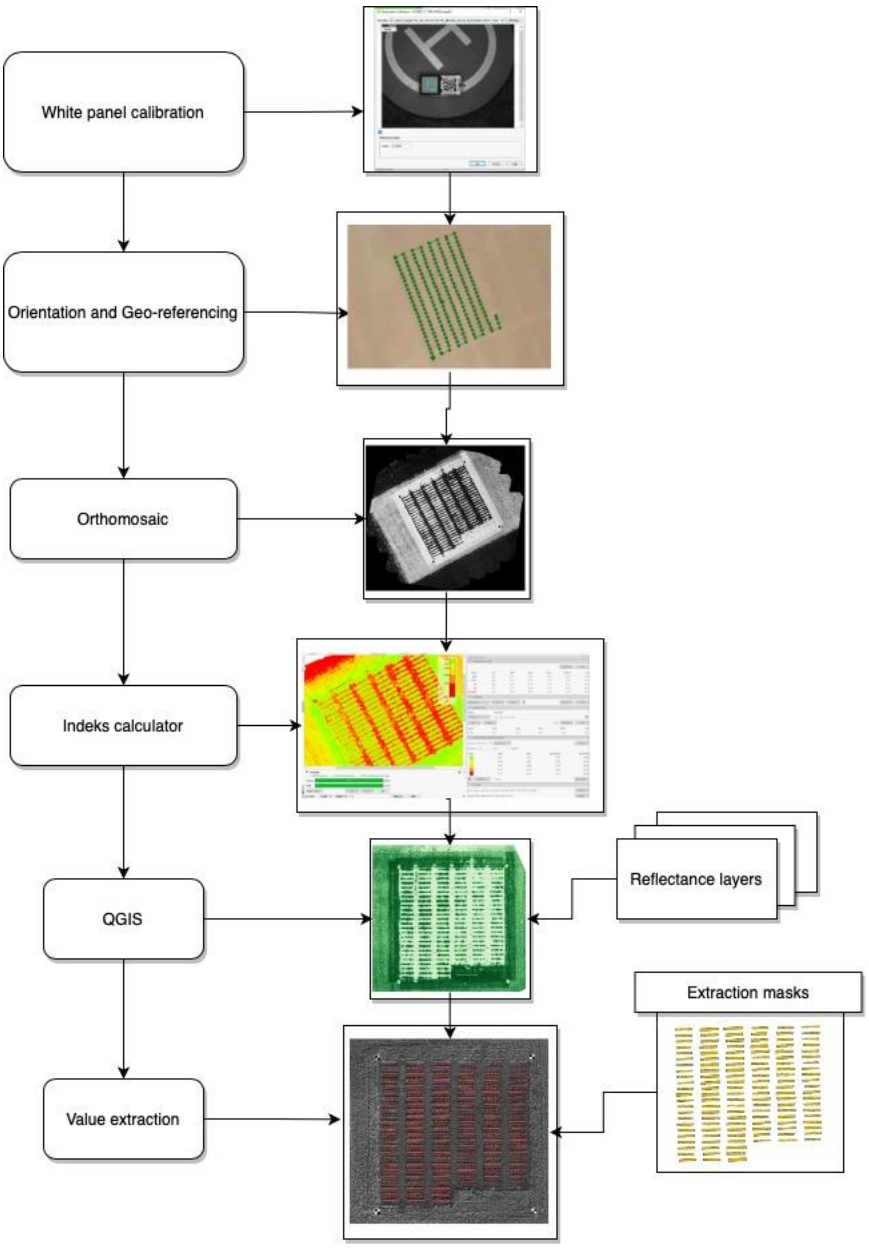

Figure 3. Workflow for the data processing in Pix4D and QGIS.

The height values used for further results and predictions are the median value from each row/plot extracted with the polygons. Which extract the values only from the extracted plot/row. All calculations are done with raster data, which is the 2D-image of each pixel. Since the exact size of each pixel (GSD) is known in meters, to estimate a volume the size of the GSD is squared to determine the area, and then the area is multiplied with the height model to get a volume in m^3 per pixel. The values that are used for further results and predictions are the sum of the volume pixels

from each extraction polygon, and some space around the row/plot to make sure all the volume is included. For this calculation, weeds between the rows/plots could therefore be a source of error. The height values are more precise. The calculations are the same for both RGB images and multispectral images from both rows and plots.

Vegetation indices:

Instead of directly using the spectral bands in crop monitoring, an interesting approach is using vegetation indices for the estimation of yield and phenotypic traits. Different vegetation indices were calculated based on their corresponding formula according to table 3.

Table 3: The multispectral indices evaluated in this study.

Indices	**Complete name**	**Indices formulation**	**References**
NDVI	normalized difference vegetation index	(NIR – Red)/(NIR + Red)	
EVI	Enhanced vegetation index	2.5*((NIR-RED)/(NIR+(6*RED)-(7.5*BLUE)+1))	(Barzin et al., 2020)
MTCI	MERIS terrestrial chlorophyll index	(NIR - Rededge)/(Rededge - Red)	(Dash & Curran, 2007)
SR	Simple ratio	(NIR/Red)	(Barzin et al., 2020)
EXGR	Excess green- Excess red		(Liu et al., 2022)
EXG	Excess Green	(2Green – Red- Blue)	(Meyer & Neto, 2008)
GNDVI	Green Normalized Difference Vegetation Index	(NIR-Green)/(NIR+Green)	(Barzin et al., 2020)

2.3.1 R-Studio R. 4.2.2 (2022-10-31) “Innocent and Trusting”, Python

The script for early statistics and sorting was made in R-Studio R. 4.2.2 (2022-10-31) Innocent and Trusting) (https://posit.co/download/rstudio-desktop/). The script was made to upload the data from the large file folder and join it into one big table. Each sample had its own unique number, which made it possible to find the exact row or plot from one specific day and height. Furthermore, the script was also made to combine the results to correlation matrix and scatterplot for the correlation. The figures, heatmaps and predictions were made in Python using Jupyter Notebook (*Jypiter Notebook*). Correlation heatmaps and predictions were done in the same way for both locations, and for all heights. For the two camera types, the only difference in the processing was that the reflectance bands were not included for RGB heatmaps and prediction.

2.3.2 Linear regression prediction model, Python

The yield predictions were done using a multiple linear regression between image data as input and DMY as output. The linear regression is fitted using the input values as the independent variable and the output values as the depended value. The correlation coefficient and the root mean squared error (RMSE) between the actual (actual DMY) and the predicted values (predicted DMY) were calculated to assess the model accuracy. The RMSE is the sample standard deviation of the differences between the predicted values and the measured (residual) values, the lower RMSE, the better prediction. The linear regression code was developed in Python.

3. Results

3.1 Phenotyping data

3.1.1 Fresh yield at Ås

The relationship between fresh weight (FW) and dry matter yield (DMY) for each diploid and tetraploid population at Ås is presented in figure 18 (Appendix 1.). The maximum variation occurs during the first cut where the FW ranges between 500g to 2000g. The average yield for diploid populations at the first cut was 1079g, while tetraploid populations had an average DMY of 652g. The average yield for both trials and for each cut presented in both FW and DMY is illustrated in figure 17. (Appendix 1.) and fully written in table 18 (Appendix 2.) The diploid trial had higher yield for all four cuts at this location. Th first cut for both trials yielded the FW of 1079.4 g and DMY of 270.3 g for the diploid trial, and FW of 651.9g and DMY of 170.9g for the tetraploid trial. The highest yield was produced in the second cut for both trials with the following results for the diploid trial: FW = 1316.9 g, DMY = 378.7 g, and for the tetraploid trial: FW = 1110.1 g, DMY = 307.7g. The third cut had a reduced yield almost to halved compared to the second cut with the following results for the diploid trial: FW = 666.6 g, DMY = 196.9 g and for the tetraploid trial: FW = 528 g, DMY = 159.2 g. The fourth cut had the lowest yield with FW of 285.8 g and DMY of 101.7 g for the diploid trial and FW of 186.8g and DMY of 70.8g for the tetraploid trial.

3.1.2 Dry Matter Percentage at Ås

The dry matter percentage of the yield from Ås is presented in figure 4. The figure shows an increased dry matter percentage for each harvest. The dry matter percentage is the average fresh yield from the whole trial, all populations combined, with the average dry matter yield for the whole trial The dry matter percentage from the first cut was 25% for the diploid and 26.2% for the tetraploid. The dry matter percentage for the second cut was 28.7% for the diploid and 27.7% for the tetraploid. The dry matter percentage for the third cut results in 29.5% for the diploid and 30.1% for the tetraploid. The fourth cut gave a dry matter percentage a bit higher than the

previously cuts, with a 35.3% dry matter for the diploid, and 37.9% dry matter for the tetraploid.

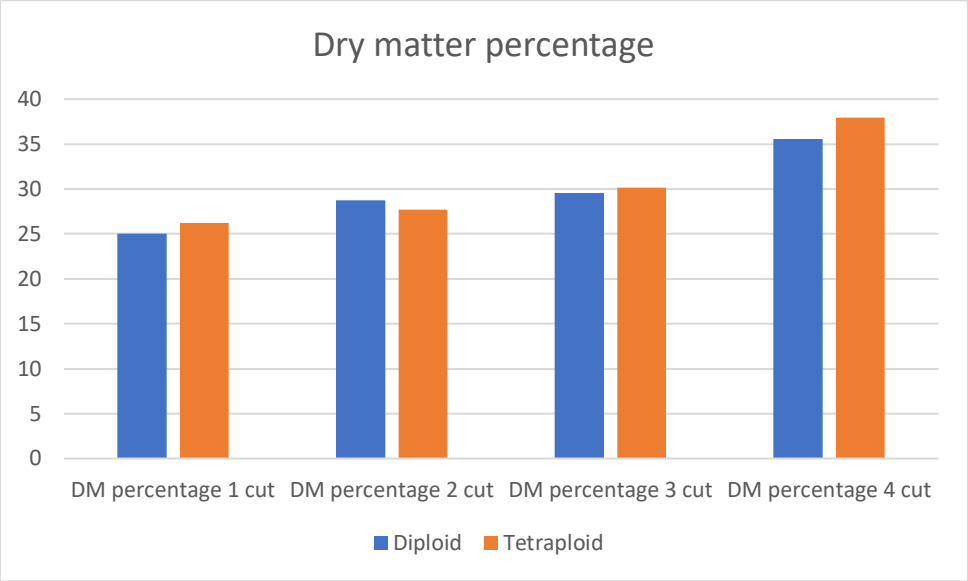

Figure 4. Dry matter percentage from rows at Ås.

3.1.3 Fresh weight at Arneberg

The fresh yield from Arneberg is illustrated in figure 15. and figure 16 (Appendix 1). The average yield from each cut from both diploid and tetraploid trials sampled as rows is pictured in figure 16 (Appendix 1). The first cut yielded the average FW of 2361 g and 3576 g, respectively for diploid and tetraploid trials. From the first to the second cut, the average yield was reduced by 34 % for the diploid trial and 31% for the tetraploid trial with FW of 1559g for the diploid trial and 2451g for the tetraploid trial. The third cut had a reduction of 53% for the diploid trial and 48% for the tetraploid trial with the fresh weight 719 g and 1254 g respectively for the diploid and tetraploid trials. The fourth cut gave a small increase in yield on 4% from the third cut in the diploid trial and with FW being 748g and the tetraploid trial had a difference on 22% with a decrease in yield from the third cut with FW being 967g.

The average fresh weight yield for both diploid and tetraploid trials, as sampled in plots, is illustrated in figure 15 (Appendix 1). The highest yield obtained from this field was from the first cut with a FW of 20739 g for diploid trial and 22277g for tetraploid trial. In the second cut there was a reduction in yield compared to the first cut. The diploid trial had FW of 12063 g, resulting

in a 41% reduction. The tetraploid trial had a FW of 14829 g, indicating a 33% reduction. For the third cut, the yield decreased even further compared to the second cut. The diploid trial had a FW of 4901g, resulting in a 59% reduction, while the tetraploid trial had a FW of 5916 g representing a 60% reduction.

3.1.4 Dry matter percentage at Arneberg

The dry matter yield from Arneberg is calculated with a NIR instrument mounted on the Haldrup harvester. Calculated percentage of dry matter compared to fresh weight is presented in Figure 5. for rows and Figure 6. for plots. As illustrated in figure 5. the dry matter percentage is higher in the diploid trial (1073) than the tetraploid trial (1074). The difference between diploid and tetraploid trial was between 3-4% overall in favour of diploid trial, but the biggest difference occurred at the second cut with 4% difference in dry matter.

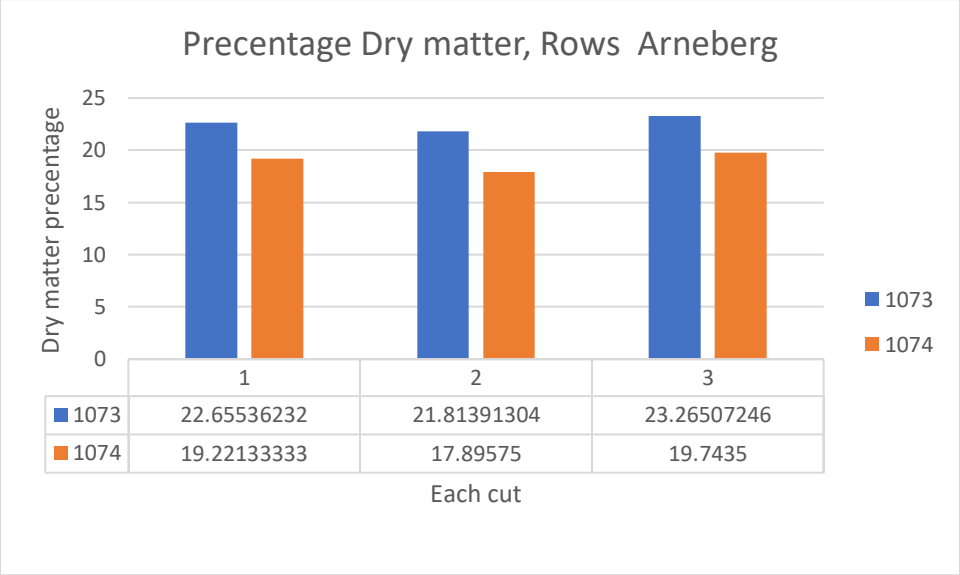

Figure 5. Percentage Dry matter from rows at Arneberg, calculated with a NIR instrument mounted on the harvester.

The plots dry matter percentage is lower compared to the rows at Figure 5. Diploid trail (1073) had higher dry matter percentage compared to the tetraploid trial (1074) for both cuts. The diploid trial had a dry matter percentage of 18,8 % for the first cut and 19% for the second cut. The tetraploid trial had a dry matter percentage of 17.4% for the first cut and 16.7 % for the second cut.

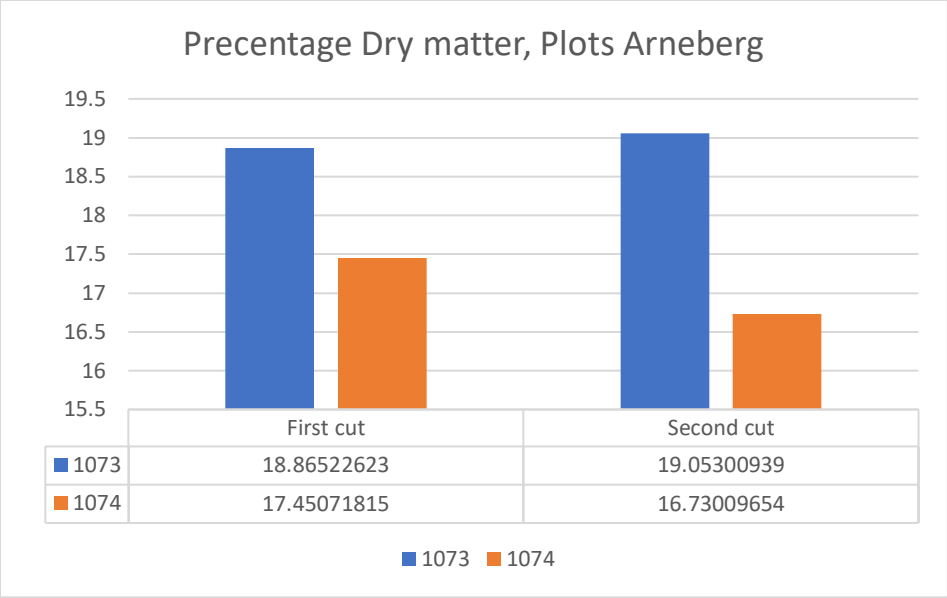

Figure 6. Dry matte percentage of plots at Arneberg, first and second cut.

3.1.5 Fresh weight yield comparison of rows and plots form Arneberg

The yield from both rows and plots from Arneberg is visualized in figure 7. and 8. The figures include yield from the first and second cut. The different populations are presented as individual colours, which are the same for both first and second cut. The diploid populations, which are the populations planted in 1073 trial (diploid trial) are presented in figure 8. Here it seems that some of the populations have similar placement on both first and second cut, such as 17-SV1-17606/1, 17-SV1-17602-1, and PH-2X. Other populations tend to have a more random distribution, between both first and second cut, but also for the yield from rows and plots. The samples are sorted in ascending order based on the plot yield. Table 17 (Appendix 2.) shows the complete

order.

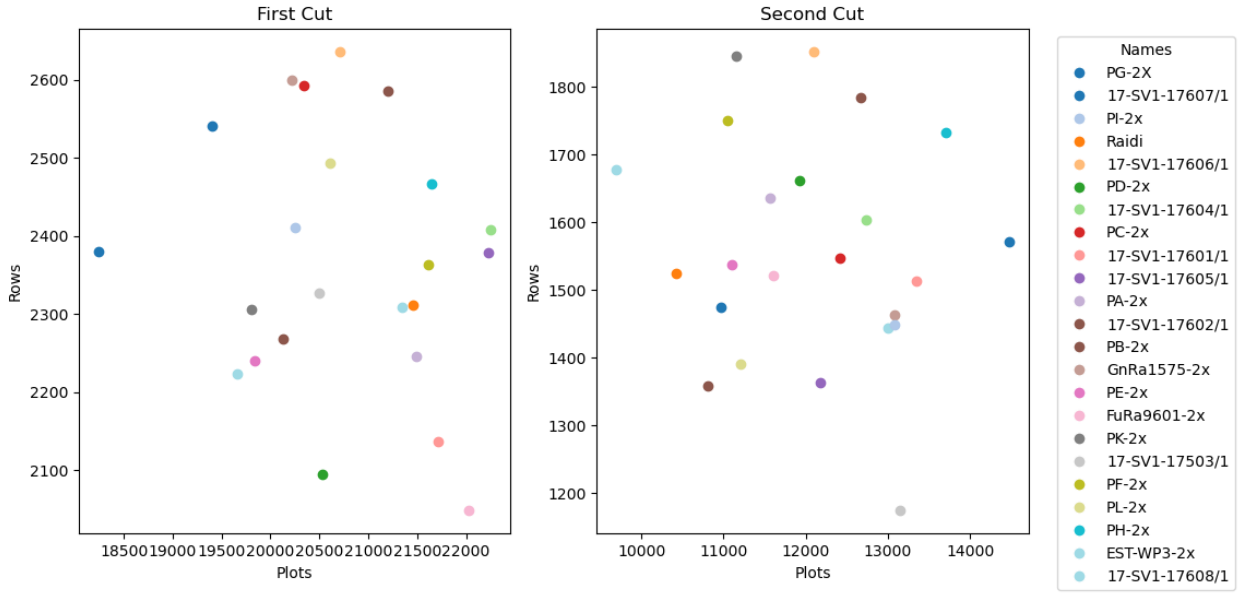

Figure 7. Comparison of yield (g) between rows and plots form diploid populations, X-axis: plots, y-axis: rows. Each population has its own colour, that is same for both cuts.

The distribution of the tetraploid populations is more randomized compared to the diploid populations, with little to none of the populations showing a repeating trend between the cuts. There is no easily visible relation between rows and plots. Some populations however have some similar positions in both scatterplots such as Fagerlin, Fagerlin+Figgjo, and PN-4x. Fagerlin had a low yield in plots for both cuts, but in the rows, the yield was higher than for other populations that performed better in plots such as PG-4x, Fagerlin+Raminta, Fagerlin+Birger, and

Figgjo+Trygve+Birger. Raminta had one of the highest yields in plots with 23296 g in the first cut and 17282 g in the second cut (table 16. in appendix 2.) but a low yield in rows.

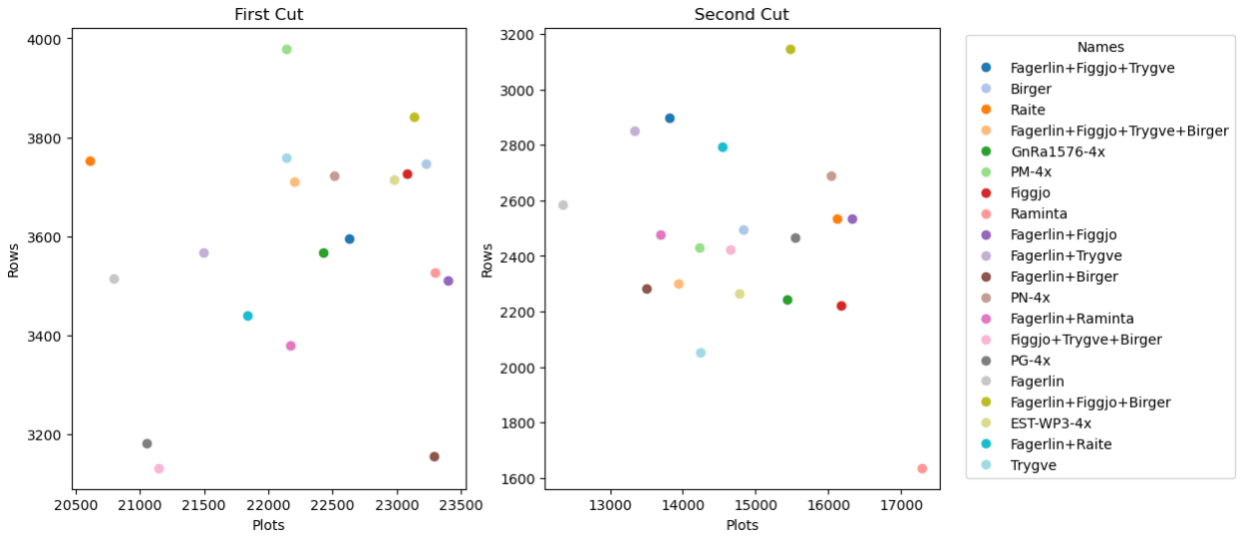

Figure 8 Comparison of yield between rows and plots for tetraploid populations, X-axis: plots, y-axis: rows. Each population has its own colour for both cuts.

3.1.6 Fresh weight yield comparison between rows at Ås and Arneberg

The fresh weight from the rows at Ås was compared with the fresh weight from the rows at Arneberg. The comparison was done separately for diploid trial (Figure 9.) and tetraploid trial (Figure 10.). The figures were generated with the average yield from each population, sorted in descending order made from the fresh yield from the first cut at Ås (table 21. and table 22. in Appendix 2.). For both trials and for both cuts, there were no visible relation between the yield of different populations at Ås and Arneberg. Only some populations indicated a trend.

The comparison for the diploid trial is illustrated in Figure 9. Based on the illustration, there is no visible relation between the populations from the different locations since many of the populations that produced a low yield at Ås gave a higher yield at Arneberg. At the first cut, one population that preformed equally low at both locations was PD-2x, however, at the second cut this population gave higher yield.

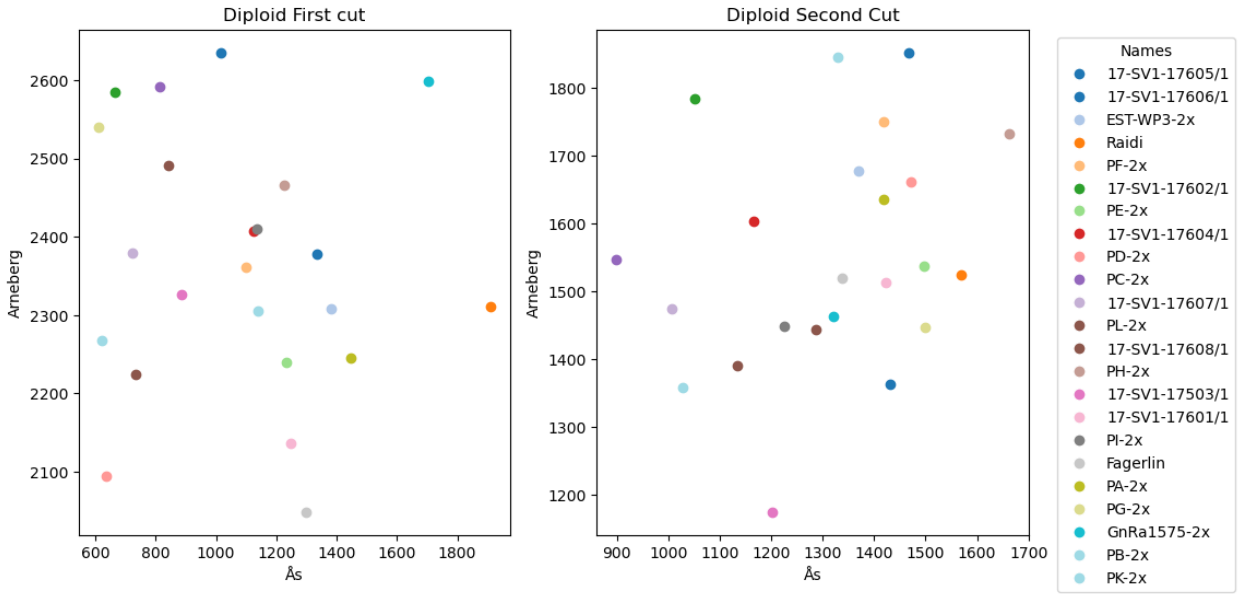

Figure 9. Comparing fresh yield from rows at both locations, diploid trial

The comparison for the tetraploid trial is illustrated in Figure 10. There is one population, PG-4x, that preform low at both locations at the first cut but better at the second cut. For the second cut, the relation between the locations forms a line and this indicate some relation between the populations. There are some populations that are off, but it's possible to see an increasing line containing the populations Trygve, Figgjo, GnRa1576-4x, Figgjo+Trygve+Birger, PG-4x, Birger, and

Raite.

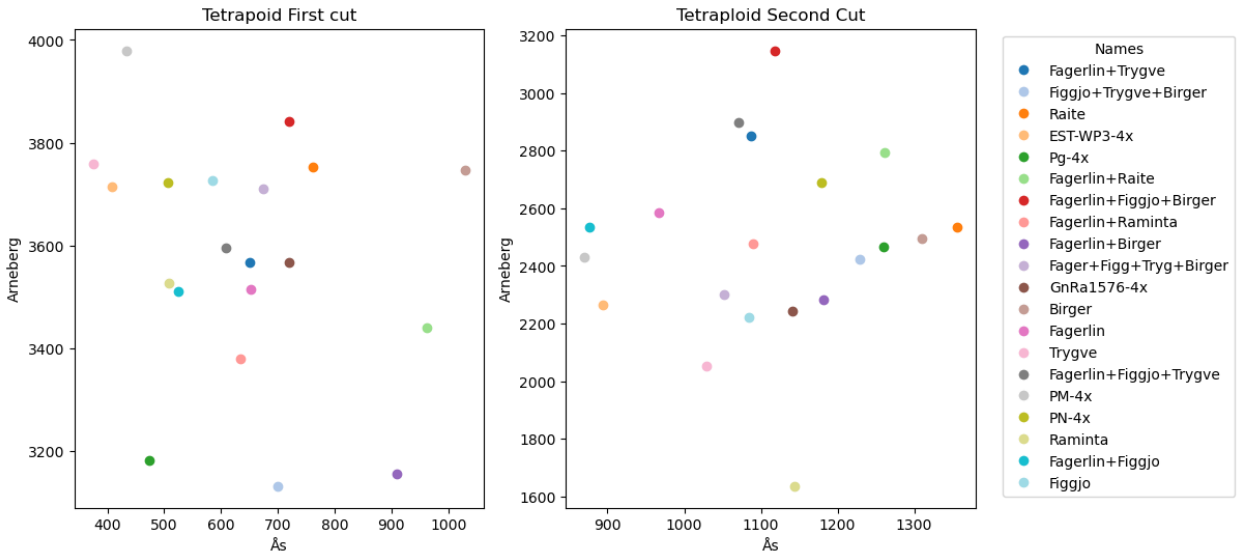

Figure 10. Comparison of fresh yield from rows at both locations, tetraploid trial

3.2 Spectral reflectance

3.2.1 The effect of ground sampling distance (GSD) or flight altitude on spectral reflectance

To study the effect of flight altitude or GSD on spectral reflectance, the results of NDVI calculations for different flight altitudes and their correlations are presented for row trial at Ås for the two first cuts (Table 4.) Images on several growth stages were included according to registrations preformed along the image data assessment (Table 19 in appendix 2.). The images inspected for GSD were taken at growth stage around heading. The assessment dates were as following: 4 days after heading prior first cut (25.05.2022), 6 days after heading prior first cut (27.05.2022), the first cut (02.06.2022), regrowth 16 days after harvest (18.06.2022), two days after heading prior second cut (25.06.2022), and one day before the second cut (05.07.2022)

The results from the image data indicated a high correlation between all heights in all inspected occasions (0.93-0.99) (Table 4.). The assessment day with the overall highest correlation in advance of the first cut is between heights from six days after heading, first cut (0.99). There is a 0.99% correlation between 30m and 50m at the day of the first cut. Before the second cut, the assessment day with the highest correlation between heights is two days after heading, with the same correlation between all correlated heights (0.98). The correlation from regrowth, 16 days after harvest, seems to have the lowest correlation between all the correlated height (0.93-0.94).

One day before the second cut has a lower correlation between the heights (0.94-0,96) compared to two days after heading (0.98).

Table 4. NDVI correlations between different heights at Ås

NDVI correlation heights	Four days after heading first cut	Six days after heading first cut	First cut	Regrowth 16 days after harvest	Two days after heading for second cut	One day before second cut
15-20	-	-	-	0.94	-	-
20-30	0.99	0.99	-	0.94	0.98	0.96
20-50	0.98	0.99	-	-	0.98	0.95
30-50	0.98	0.99	0.99	-	0.98	0.94
15-30	-	-	-	0.93	-	-

3.2.2 Correlation between multispectral UAV-image data and yield from rows, first and second cut at both locations

The image data were assessed throughout the season, with several flights before both first and second cut. Since the image data were captured from different flight altitudes and the results (table 4) showed little to almost none difference between the heights, the stages with the highest correlation between heights were investigated further for correlation between yield and multispectral data (four days after heading before the first cut, six days after heading before the first cut, the day of the first cut, and two days after heading before the second cut).

Pearson correlation between spectral bands and some vegetation indices calculated at different flight altitudes are presented in Table 5. the Red-edge showed the highest correlation of 0.80 with

DMY acquired at 30 meters for the day of the first cut. The highest NIR correlation equal to 0.86 was observed at four days after heading and the day of the first cut. This indicates that the highest correlation between yield and UAV-images was from the images taken the day of the first cut. The visible reflectance bands showed a negative correlation with yield. These reflectance bands however are still used for calculating of VIs in the next step of processing. The highest correlation between NDVI and DMY was acquired from six days after heading before the first cut with a correlation of 0.80 (for 50 meters) and 0.79 (for 30 meters).

The correlation heatmap from six days after heading and before the first cut (27.05.2022) is presented in figure 11. Here the lowest line is the dry matter yield, while the line above is the fresh yield. These two yield measurements had a correlation coefficient on 0.98. The maximum correlation between any VI and the yield occurs between the dry matter yield and MTCI with a correlation on 0.87. A high correlation with MTCI indicate an increase in chlorophyll content. Other VIs with a high correlation with the dry matter yield is NDVI = 0.80, NIR = 0.83, GNDVI = 0.84 and SR = 0.86. Measured volume has a correlation with the dry matter yield on 0.84.

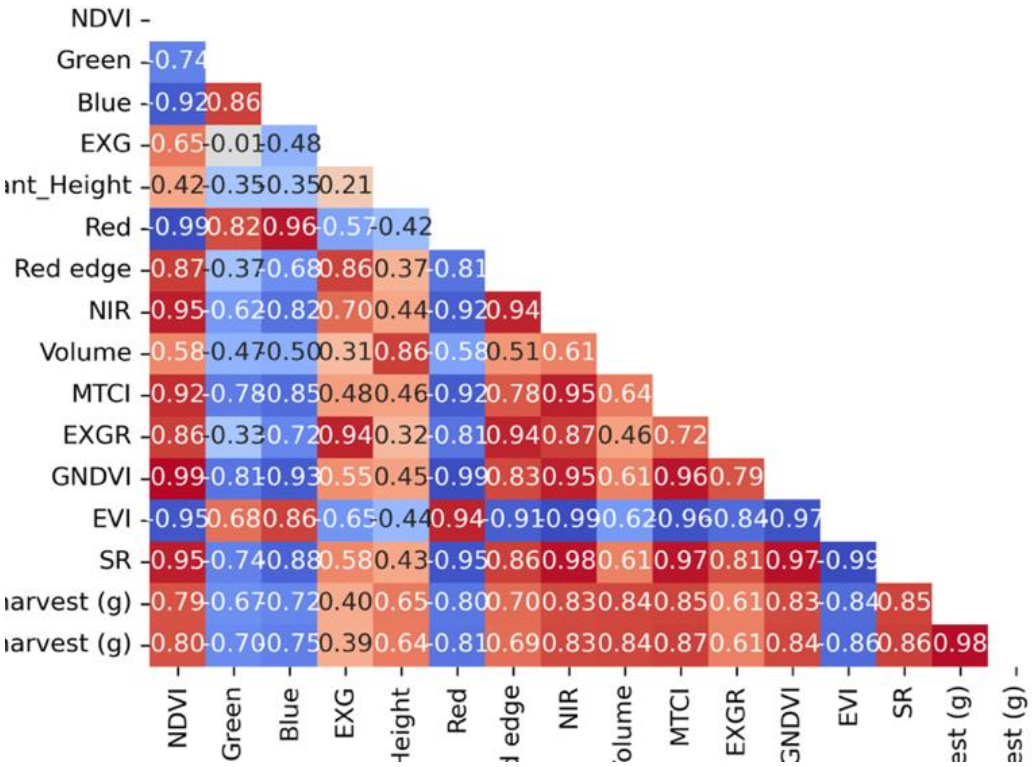

Figure 11. Correlation matrix from multispectral data at 27-05-2022, at 30 meters and for yield from first cut.

Table 5. Correlation values between reflectance indices and DMY values, first and second cut, rows at location Ås.

Assessment day	Four days after heading first cut			Six days after heading first cut			First cut		Two days after heading for second cut		
Altitude	20m	30m	50m	20m	30m	50m	30m	50m	20m	30m	50m
Red-edge	0.70	0.79	0.77	0.71	0.70	0.68	0.80	0.79	0.16	0.07	-0.20
Red	-0.60	-0.64	-0.65	-0.70	-0.80	-0.79	-0.64	-0.68	-0.36	-0.36	-0.47
NDVI	0.65	0.77	0.67	0.79	0.79	0.80	0.76	0.78	0.49	0.50	0.52
NIR	0.78	0.86	0.81	0.83	0.83	0.83	0.86	0.86	0.44	0.38	-0.05
Green	-0.30	-0.10	-0.07	-0.65	-0.67	-0.65	-0.16	-0.23	-0.17	-0.14	-0.32
Blue	-0.45	-0.18	-0.53	-0.70	-0.72	-0.71	-0.25	-0.34	-0.21	-0.21	-0.32

The correlations between reflectance bands and yield of rows at Arneberg (captured at 20 meters flight altitude) is presented in table 6. This table includes two assessment dates before the first cut, 25 days before first cut (19-05-2022), and 20 days before first cut (24-05-2022) as well as the day of the first cut (13-06-2022). For the second cut, the two assessment dates of 18 days before the second cut (25-06-2022) and five days before the second cut (08-07-2022) were selected. Based on the results in table 6, the red edge and NIR exhibited the maximum correlation of 0.80 and 0.67 respectively in 25 days before the first cut however the NDVI Showed a negative correlation in this capture date. NDVI exhibited a positive correlation of 0.41 for 18 days before the second cut.

Table 6. Correlation between reflectance indices and DMY, first and second cut, rows at Arneberg, 20 m height.

Assessment date	25 days before first cut	20 days before first cut	First cut	18 days before second cut	Five days before second cut
NDVI	-0.27	-0.21	-0.31	0.41	-0.44
Green	0.39	0.53	0.48	0.18	0.08
Blue	0.35	0.62	0.72	0.21	0.41
Red-edge	0.80	0.70	0.40	0.41	-0.22
NIR	0.67	0.66	0.49	0.47	0.06
Red	-0.06	0.44	0.59	0.03	0.55

The correlations between reflectance indices and DMY values from the Arneberg plot trials is presented in table 7. The same assessment dates as for the rows were investigated including: 25 days before first cut, 20 days before first cut, first cut, 18 days before second cut, five days before second cut, as well as one day before the second cut (12.07.2022). The results from the plots also include both hights that was used at location Arneberg (15m and 20m). In these results, the best correlation for the first cut was 20 days before the first cut, captured at 20 meters. For the second cut, the best correlation was five days before the second cut, captured at 15 meters. Both heights at five days before the second cut had a NDVI correlation at 0.20, but slightly different values for the other reflectance bands.

Table 7. Correlation between reflectance indices and DMY from first and second cut fromplots at Arneberg, 15 m and 20 m height.

Assessment date	25 days before first cut		20 days before first cut		First cut		18 days before second cut		Five days before second cut		One day before second cut	
Height (m)	15	20	15	20	15	20	15	20	15	20	15	20
NDVI	-0.02	-0.21	-0.03	0.25	0.02	-0.05	0.09	-0.41	0.20	0.20	0.14	0.36
Green	0.04	-0.12	0.04	-0.34	0.03	0.12	0.11	0.22	0.19	0.18	-0.02	-0.34
Blue	-0.04	-0.31	0.04	-0.40	0.01	0.10	-0.16	0.29	0.07	-0.17	-0.05	-0.43
Red-edge	0.04	0.08	0.04	0.13	-0.01	0.11	-0.03	-0.09	0.28	0.30	0.02	-0.33
NIR	0.03	0.08	0.03	0.13	0.01	0.09	-0.01	-0.19	0.36	0.19	0.10	-0.33
Red	0.14	0.02	-0.26	0.03	0.04	0.16	0.14	0.38	0.08	0.30	-0.21	-0.39

3.2.3 Correlation between volume measured from RGB camera and DMY from first and second cut at both locations

The correlation between volume measured and calculated with RGB images and yield is illustrated in table 8. The correlation from location Ås is done by correlating volume data measured at the same day as both the first cut (02.06.2022) and the second cut (06.07.2022) but at four different altitudes,15-meter, 20-meter, 30 meter and 50 meters correlated with the yield measured as fresh weight for the same location.

The correlation for the first cut shows a very high correlation at the lower altitudes. The highest correlation, which was 0.91, was observed between volume measured at 15 meter and the actual yield from the first cut. The correlation between RGB measured volume from 20 meters and yield was 0.90. For 30 meters, the correlation coefficient was 0. 87, and for 50 meters the correlation coefficient was -0.12. The correlation between volume and the yield at second cut was lower compared to the correlation at the first cut. The correlation coefficient at the second cut was 0.83 for all altitudes. This indicates a strong relation between the images from the different heights, and the yield measured from this date.

Table. 8: Correlation coefficient between volume measured by RGB camera, and yield harvested at first and second cut at Ås

	First cut	Second cut
15 meters	0.91	0.83
20 meters	0.90	0.83
30 meters	0.87	0.83
50 meters	-0.12	

The correlation between RGB measured volume and yield from plots at location Arneberg is presented in table 9. Here the results are very poor and indicate almost no correlation at all. This is consistent for all assessment dates in plots for the RGB images. The same results have been observed in rows as well with the same camera.

Table 9. Correlation coefficient between volume measured on plots by RGB camera, and yield. at Arneberg

Flight dates	25 days before first cut	20 days before first cut	Date of the first cut	18 days before the second cut	Five days before the second	One day before second cut
15 meter	0.05	0.04	0.00	0.03	0.00	0.06
20 meter	0.05	0.04	0.00	0.03	0.00	0.06

3.2.4 Correlations between UAV-images with vegetation indices and DMY from rows at both locations

The correlation between VIs from multispectral images and DMY from rows at Arneberg and Ås is presented in table 10 and table 11. The data from Ås is from 20 meters, 30 meters and 50 meters (table 10.). The data from Arneberg is presented in table 11. And are from rows with multispectral images captured at 20 meters.

Vegetation indices that are included in these correlations are described in table 3.

- Excess Green (EXG)
- Meris Terrestrial Chlorophyll Index (MTCI)
- Excess Green minus Excess Red (EXGR)
- Green Normalized Difference Vegetation Index (GNDVI)
- Enhanced Vegetation Index (EVI)
- Simple Ratio (SR).

The dates that were presented here are the same assessment dates that correlated the most for each cut on both locations, presented in table 4. and 5. The chosen date from location Ås was four days after heading (25-05-2022) for the first cut, and two days after heading (25-06-2022) for the second cut. Results indicate a slightly higher correlation with 50 meters at the first cut compared to 30 meters. While the correlation at the second cut had lower correlation for all heights compared to the first cut. VIs that correlated good with DMY was SR, NDVI, MTCI, and GNDVI, they all had a correlation coefficient above 0.80.

Table 10. Correlation coefficient between DMY and VIs from multispectral images before first and second cut at Ås

VI	Four days after heading prior first cut		Two days after heading prior second cut	
Altitude (m)	30	50	30	50
SR	0.84	0.85	0.45	0.46
NDVI	0.78	0.80	0.49	0.51
EXG	0.48	0.67	0.11	-0.21
MTCI	0.82	0.84	0.35	0.29
EXGR	0.65	0.74	0.30	-0.08
GNDVI	0.81	0.81	0.37	0.40

EVI	-0.87	-0.87	-0.56	-0.36

When looking at the correlation coefficient between reflectance bands, VIs, and yield from location Arneberg (table 11.). The correlations are higher at 25 days before first cut (19-05-2022) for some of the VIs such as SR, NDVI, EXG, and EXGR. The correlations from 18 days before the second cut (25-06-2022) have higher correlations on Vis such as MTCI and GNDVI.

Table 11. Correlation coefficient between reflectance bands, VIs, and DMY from 25 days before first cut and 18 days before the second cut captured at 20 meters from rows at Arneberg

VI	25 Before first cut	Before second cut
SR	0.39	0.34
NDVI	0.40	0.36
EXG	0.44	0.26
MTCI	0.19	0.38
EXGR	0.57	0.31
GNDVI	0.29	0.35
EVI	-0.55	-0.36

3.2.5 Correlation between UAV-images, VIs, and DMY from plots, first and second cut

The correlation between UAV-images, vegetation indices (VI) and yield from the plots at location Arneberg gave poor results for both first and second cut. With the reduces number of flights, ~~wa~~ was only possible to correlate UAV-images from 15 and 20 meters with yield. The results gave very low values, which indicated no correlation at all. Some of the results indicated even a high

correlation between the yield from the second cut with dates before the first cut which should not be occurring.

3.3 Regression analysis

3.3.1

Predictions of DMY was done by combining multispectral reflectance values, and VIS as well as prediction using UAV-based calculated volume and height using RGB images from different heights.

Table 12 presents the predictions of dry matter yield (DMY) from the Ås location. The prediction for the first cut, made 9 days prior to the actual cut (02-06-2022), was more accurate compared to the prediction for actual cut. The correlation coefficient (r) for predicted DMY on 25-05-2022 was 0.92, while for the predicted DMY on 02-06-2022 it was 0.9.. From the chosen dates, it can be observed that 9 days before the first cut (four days after heading, 25-05-2022) had the highest correlation with yield from the first cut. Although there was a small difference between the heights in terms of the predicted DMY, the overall prediction was still quite high, as indicated in Table 12.

Table 12 includes the predictions for the second cut at the Ås location. The prediction for the second cut was based on images taken at specific dates: 16 days after the first cut (18-06-2022), 11 days before the second cut (25-06-2022), and one day before the second cut (05-07-2022). Among these predictions, the height that yielded the best was 50 meters, with a prediction with r value of 0.81 for the prediction made 2 days after heading for the second cut (25-06-2022). Additionally, a prediction using a height of 15 meters was included for the second cut, although only one date was available, which corresponded to the regrowth 16 days after the first cut (18-06-2022). Nevertheless, this prediction also exhibited a high correlation with an r value of 0.80. All predictions for the second cut were generally lower compared to the first cut. However, there is a high level of consistency among predictions, and the different heights and dates showed similar trends.

Table 12. Correlation Coefficient (r) for DMY prediction for location Ås, using both spectral bands and VIs

Assessment day	Four days after heading first cut	6 days after heading first cut	First cut	Regrowth 16 days after first cut	2 days after heading for second cut	One day before second cut
15 meters	-	-	-	0.80	-	-
20 meters	0.91	0.89	-	0.79	0.76	0.67
30 meters	0.92	0.92	0.90	0.79	0.78	0.65
50 meters	0.92	0.91	0.90	-	0.81	0.75

The DMY prediction with calculated volume and height using RGB images for location Ås is presented in table 13. The best prediction with this camera type was performed with images from 15 meters, especially for 20 days before the first cut (14-05-2022) and one day after heading (22-05-2022) before the first cut. The earliest date was 20 days before the first cut (14-05-2022) but this date gave the highest prediction with a correlation coefficient on 0.92.

Table 13. Correlation Coefficient (R) for DMY prediction from location Ås, Volume and plant height from RGB.

Assessment day	14 days after growth registration	One day after heading, first cut	Regrowth 16 days after first cut	Second cut
15 meters	0.92	0.87	0.77	0.69
20 meters	0.86	0.85	-	0.70
30 meters	-	0.79	0.64	0.72

Figure 12 shows the scatter plot of the predictions for the first cut (with images captured at 50 meters) which proven to be the best prediction with r value of 0.92. This is a similar result as prediction made from images captured at 30 meters.

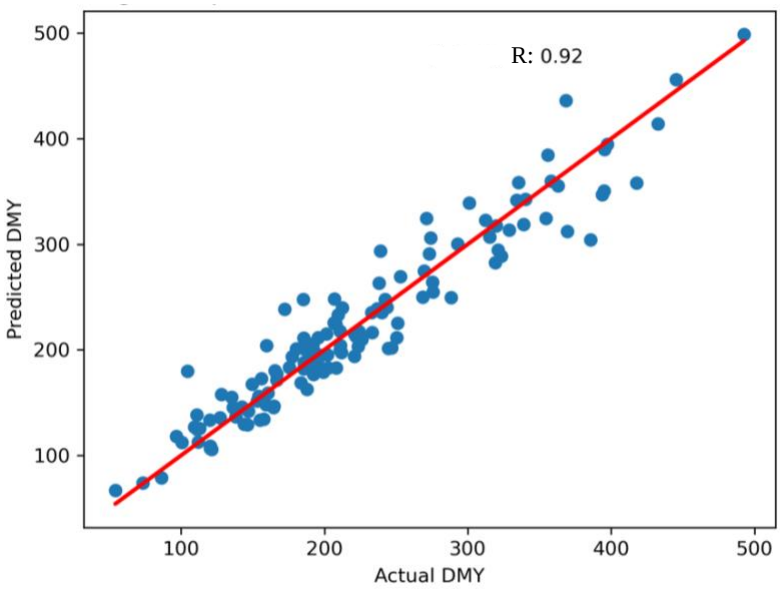

Figure 12. Prediction of DMY from rows at Ås, captured at 10 days before the first cut (25-05-2022) 50 meters

3.3.2 DMY prediction using multispectral and RGB images for rows and plots at Arneberg

Table 14 displays the dry matter yield (DMY) predictions obtained for the Arneberg location. It is observed that the predictions made before the first cut (13-06-2022) were higher compared to those made five days before the second cut (08-07-2022) and preceding dates. The difference between the predictions for these cuts was 0.15. The highest prediction was at 25 days before the first cut (19-05-2022) with a prediction of 0.74. There was a difference of 0.15 between the predictions for these cuts. Notably, the highest prediction was achieved at 25 days before the first cut (19-05-2022) with a value of 0.74. This particular date has previously shown a strong correlation with yield in both reflectance bands (Table 7) and vegetation indices (VIs) (Table 11).

Table 14. Correlation Coefficient (R) for DMY Prediction from location Arneberg, Rows

Assessment day	25 days before first cut	20 days before first cut	Date of the first cut	18 days before the second cut	Five days before the second
20 Meters	0.74	0.65	0.62	0.53	0.47

The DMY prediction for plots in Arneberg, is presented in table 15. Due to error in the RGB images, the measured and calculated volume and plant height was excluded in the regression model and prediction. The results showed a lower prediction accuracy for the first cut compared to the second, and both heights were identical at this point, r = 0.25 (25 days before the first cut), r = 0.23

Table 15. Correlation Coefficient (R) for DMY prediction from location Arneberg, plots. Multispectral without RGB data

Assessment day	25 days before first cut	20 days before first cut	Date of the first cut	18 days before the second cut	Five days before the second
15 meters	0.25	0.23	0.19	0.43	0.44
20 meters	0.25	0.23	0.19	0.38	0.55

(20 days before the first cut), r = 0.19 (Date of the first cut). For the second cut, the different heights generated different results. Where the closet to harvest, 20 meters, yielded the best prediction with r = 0.55 (five days before the second cut).

The best prediction for location Arneberg is visualized in Figure 13. The prediction is from the first cut and indicate a prediction that explain 74% of the actual DMY with the measured DMY from UAV-images.

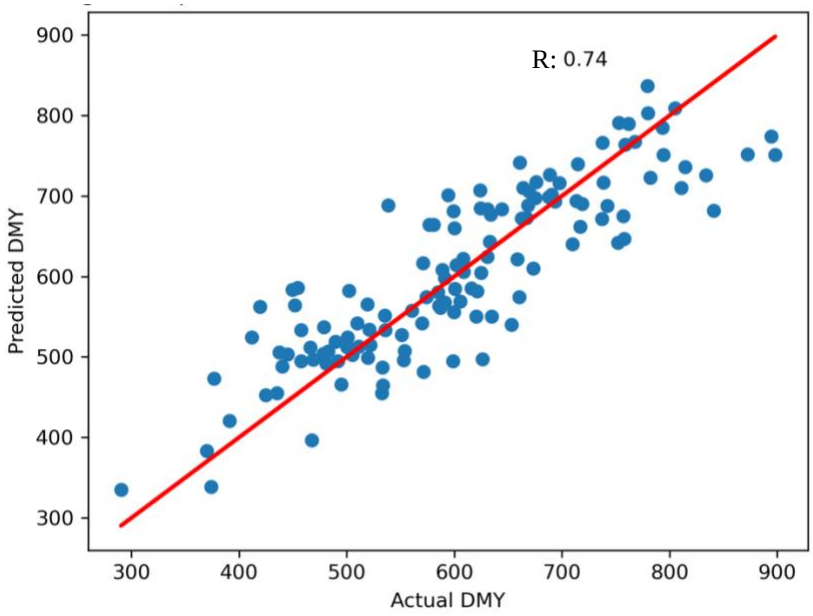

Figure 13. DMY prediction from 27 days before the first cut (19-05-2022), Location Arneberg, 20 meters.

4.Discussion

4.1 Phenotyping data

4.1.1 Yield from Ås

The results for the yield-data from location Ås indicates that the highest yield from both trials were from the second cut, the trial with the highest yield was the diploid trials for all harvests throughout the season.

The yield from location Ås was higher in the diploid trial compared to the tetraploid trial, this outcome is different than location Arneberg where the highest yield was collected from the tetraploid trials for both plots and rows in all cuts. A higher yield for the tetraploid trial is expected according to previous studies (Kemesyte et al., 2017; Pranga et al., 2021) An explanation for this result at location Ås could be the fact that the tetraploid trial was placed in the upper part of a small hill, and the diploid trial was placed at the bottom. The small hill mentioned has a hight difference of 1 meter on the diagonal (Nibio). It may be a source of error with the possibility that the tetraploid trial may have experienced drouth, or lack of nutrients and fertilizer compared to the diploid trial. Based on our experience after data assessment and constantly observing the filed through the season, it was clear that the yield from tetraploid was lower in comparison to the diploid trial. Other factors such as weeds and drouth signs was similar all over the field for both tetraploid and diploid repetitions. And all other treatments were the same for both trials. Since the data doesn't give any clear reason for the unexpected yield result, and our other results don't give an explanation, it's not possible to tell why this yield result occurred. Respectfully it does not affect the prediction much since the predictions are performed on the trials separate, the results from one trial will not make an impact on other trials. This field is planned to stay for 3 years, and the 2022 season was the first harvest season for the trial, the yield-results could therefore change to the next season 2023, where there is an expectance of increase in yield (Wingan, 1995) if the ryegrass survive the winter (Leraand, 2018). One observation we did through the season was that the tetraploid trial seems to have a slower start but will catch up with the diploid trial during the season (figure 18. In Appendix 1) When looking at the dry matter percentage from Ås (figure 4) both trials look very similar, as well as the first three cuts being very similar in results. The fourth cut

however had a much higher dry matter percentage compared to the previously cuts, and when looking at the values of yield, it is a very low yield.

A reason for this could be that when weighing the yield both before and after drying, the weight of the sample bag could be included. While the water content of the ryegrass would decrease while drying, the added weight from the bag would be consistent. And estimated weight of the bag is approximately 25 grams, and some of the smallest samples from the fourth cut had a dry weight on 48 grams. This however is a consistent error for all of the cuts since the bag was included for the weighting of all cuts. Therefore, the possible added weight of the sample bag would be consistent, and possible to remove from the end results.

4.1.2 Yield from location Arneberg

The results from Arneberg indicated a higher yield at the first cut for both trials and for both rows and plots compared to the other cuts, as well as to yield at Ås. At Arneberg, the trial with the highest yield was the tetraploid trial (1074) for both rows and plots.

The yield from the row trial at Arneberg was higher than the yield at Ås. Even though the trial was similar, and the cultivars were the same, one of the major differences between Ås and Arneberg was between the yield from the tetraploid trial and a diploid trial 1073.

A possible explanation for the difference between the two locations could be an abiotic factor such as number of rainy days. The number of rainy days is almost the same for both locations with107 rain days at location Arneberg and 105 rain days at location Ås (*Ås værstasjon*, 2023). Both locations also had a soil classified with high quality soil for plant production (NIBIO, 2023). Although Ås is located more south than Arneberg, the yield is not higher.

The yield from the plots where just conducted for three cuts while the fourth cut only being taken at the rows. Reason for the lack of the fourth cut of the plots are simply because the yield became so small and the harvester (figure 19. In Appendix 3.) was not able to properly harvest and weight the yield accurately.

For a more precise and truer to reality result, is the yield measured in dry matter yield (DMY).

For the dry matter percentage in plots, results present a dry matter percentage from the first and second cut (figure 6.). Similar to the dry matter from the rows (figure 5.) the diploid trial had a higher dry matter percentage compared to the tetraploid trial. The dry matter percentage is slightly lower for the plots compared to the rows, which can be due to the data being presented by mean values for the whole trial. Some of the plots could therefore have a high variation within the plot due to small differences in the soil or other differences. This could make an impact on the total value if the variation is very high. However the trial setup with three replications are design to reduce the impact of these types if erros. . Even though the yield is reducing with each cut, the dry matter percentage is remaining similar, which could indicate that by the time of harvest, the grasses were in approximately same stage of heading with a similar water content remining in the plant. This indicate a stable DMY in both the diploid and the tetraploid populations regardless of a reduced fresh yield. Since yield is one of the most important traits in forage grasses, a stable DMY would therefore be an aim for breeding programs. The reason that a stable and predictable DMY is an important trait for the forage grasses is that this is what the farmers base their animal feed on. The total yield and its DMY determine how much the farmers have in storage for the upcoming winter season, and how feed it actual is in the gras.

4.1.3 Comparison between rows and plots at Arneberg

To compare the yield from plots and rows will tell something about the comparability of the study, since the plant material, trial setup, location and environment has been the same. However, the comparison between the yield from both plots and rows show a poor relation. The comparison also shows a poor relation between the same populations and the distribution of these in the different cuts throughout the season.

The distribution of each population between each cut is not as surprising, since that is one of the traits that the populations will be selected based on how well the different populations regrow after a harvest. This trait will vary from population to population depending on many factors that has an impact on the total yield, such as number of tillers, growth habit, phenological stage, and weeds, to mention some. One big impact on the yield, and which also could impact the results of the distribution is that this yield is from the first year of harvest. Since some populations has a lower regrowth and a slower establishing due to this being some of the breeding traits and this trial

includes several different populations. The data presented in these results is from the first year only, there is no possible way to determine how the yield will distribute next year. There could be no difference, but it is safe to assume that there will be some changes in the distributing since earlier research show an increase in yield for the second year (Marum, 2016). It needs more results to make a more precise comparison, so there should be done some comparison between rows and plots from more than one year.

Previously, Norwegian research has concluded that the meadow needs time and years to establish a stable yield, and that the number of seasons with harvest before ploughing and resowing should in fact be increased since the yield will stable itself and even increase after some years (Hind, 2020) This however is for pastures sown with a mixture of several different species for an optimal yield combination with regrowth, coverage and protein content in mind, as well as the use and location (Repstad, 2023). However, they found out that after 50 years without ploughing, the meadow included 60 % of initially sown species such as perennial ryegrass, timothy, and meadow fescue. (Hind, 2020) They also found out that the yield was higher and more stable in the old meadow compared to a similar four-year-old meadow. However, this is not typical for the forage production since the meadow often will be ploughed again after four to six years due to lower yield and production plan on the farm. With this in mind, the trial and results from this year should be replicated and tested over more seasons for a more optimal result for decision making.

4.1.4 Comparison between yield from rows at both locations

As mentioned in the previous chapter (4.1.3 Comparison between rows and plots at Arneberg) a reason for this could be that since the yield is from the first harvest season, the yield is expected to have more variation than for the next seasons (Brereton & McGilloway, 1999). When comparing the results from this comparison and the comparison between rows and plots from location Arneberg, it seems that the populations were more similar to each other in rows. This indicate that the sample size (rows or plots) affects how the populations behave and how they are observed.

4.2 Spectral reflectance

To proceed with suggesting a protocol for UAV- based phenotyping of forage grass breeding, there are some factors to inspect. This study has been using a premade schedule for image-data assessment (table 1). This schedule and protocol have been made based on results and protocols

from similar trials. (Castro et al., 2020; Gebremedhin, Badenhorst, Wang, Giri, et al., 2019; Gebremedhin et al., 2020) The flight schedule includes the flying altitude, the camera type, camera angle, image overlap and assessment time. Since one of our objectives was to determine the optimal flight height for yield prediction with UAV imagery, four different heights, were tested. However, not all dates included flights from all the four heights (15m, 20m, 30m and 50m) and both camera types. We had fewer flights with RGB camera and multispectral camera at 15 meters. It's still possible to determine how well 15 meters correlate with yield.

4.2.1 NDVI correlation

Very high correlation was observed between NDVI values calculated at different flight altitudes indicating that the flight altitude or GSD is not affecting the final calculated values. This results are in agreement with the results obtained for wheat in a recent study (Klaseie, 2022). However, the prediction results and correlations with DMY varied slightly between different flight altitudes. The NDVI (Normalized Difference Vegetation Index) is a calculated index based on red and NIR. reflectance (NIR-Red/NIR + Red) which indicates the plant health. Healthy vegetation with a lot of chlorophyll will reflect more near-infrared (NIR) and green light compared to other wavelengths, but it will also absorb more red and blue light. The results from this formula will give a result between -1 and +1. So, if the reflectance is low on red, and high on NIR, this will give a high NDVI value, and vice versa. (GisGeograpy, 2023). That means that even if the altitudes give us different outcome on other bands, the NDVI value is still valid since the actual chlorophyll content in the rows are the same, and the NDVI value is a calculated index based on the relationship between other bands. So, if the different between altitudes are consistent, the NDVI value will have a minimal variance. In this experiment, NDVI or high content of chlorophyll will tell us something about the among of forage grass in each row since the data is extracted from a defined area including only the rows.

The correlation between NDVI values from different heights is increasing closer towards the first cut, a reason for this could be when the green mass is increasing due to growth, and the reflectance become more even despite the altitude, and therefore the NDVI value will behave similarly and be more accurate.

For the correlation between the different heights towards the second cut, the NDVI correlations is lower compared to the first cut. The correlation is at its highest ten days before the second cut, and then goes down on the day for the second cut. This is not similar as for the first cut where the correlation just increased closer and closer to harvest. The reason for this outcome can be due to some changes in weather that day with more or less sun at the flight time, or some errors in the processing afterwards. But even if the correlations are lower compared to the first cut, the same tendency of a higher correlation between altitudes closer in range is still clearly visible for this period as well.

4.2.2 Correlation coefficient between reflectance bands from multispectral images and DMY from Ås

The results from the correlation between the multispectral UAV-images and yield for Ås trial indicated a high correlation between NDVI, NIR and red edge correlated DMY. The highest correlation occurred 6 days after heading before the first cut, as well as the cutting day. A lower correlation was observed for the second cut, and in general lower~~lower~~ correlation for lower flight altitudes.

The reflectance with the highest correlations is directly related to chlorophyll, since the red-edge shows the reflectance values for spectra range between 680 and 780 nm, and are caused by the combination of the effect from strong chlorophyll absorption in the red wavelengths (650 nm) and leaf internal scattering in the NIR wavelength (750-2500 nm) (Horler et al., 1983; Ren et al., 2011) a higher chlorophyll content will cause less red-reflectance and more red-edge and NIR. The expected chlorophyll content should be increasing closer to harvest since the biomass is increasing, and these results indicates the highest chlorophyll content is at the day of the first cut. However, there seems to be the same value of chlorophyll at four days after heading for the first cut captured from 30 meters. This occurs to be a strange outcome, but could be explained with changes in the weather, such as clouds shadow, wind making movements in the grass or a different time of day when flying. The capturing height for the images seems to have a positive effect on the correlations. This finding contributes to the aim of this study with the possibility to focus on the higher heights for yield prediction.

For the second cut, the correlation has drop in value, and there seems to be a strange change of value for red-edge for the second cut, but this could be related to the low values for the other indices as well, as well as the lower correlation between the heights discussed in 4.2.2 (NDVI correlation).

4.2.3 Correlation coefficient between volume from RGB camera and DMY from Ås

The results from the correlation between volume measured by RGB camera and DMY indicates a higher correlation between the yield and the volume measured by images captured at a lower altitude. The correlations between the yield from the first cut and the measured volume is significantly declining with each height, with a negative correlation at 50 meters. The declining of correlation is expected due to a lower resolution with higher flights with a RGB camera (Joyce, 2022).

This could be because the plant volume is at its largest, and therefore easier to determine even for a higher altitude. This tells us that several flights with different heights at the harvest day is not necessary since the values from this date are so similar. With the results from this correlation, the information indicates that the relationship between volume from RGB camera and ryegrass yield is very accurate for the lowest altitudes. These findings are expected since the resolution would be higher since the UAV are flying lower, and the camera would be closer to ground, and each pixel would contain a smaller area. This results in more details for the end image.

The correlation between UAV-images and yield from the plots at location Arneberg yielded very poor results and made it impossible to compare rows and plots to each other as mentioned earlier. One reason for these poor results could be due to low quality UAV-images due to camera type or changes in imaging angle. This would make a huge impact on the image-quality and could definitely be a reason for poor results. This is a highly plausible reason, since the image data from Arneberg has been over all lower compared to Ås, despite the fact that Arneberg had a significantly higher yield. Since the number of flying heights was reduced at Arneberg, the only heights to inspect are 15 meters and 20 meters. This does not necessary mean that the data from the missing heights 30 meters and 50 meters would be better, since the data from 20 meters at rows from Ås

was still significantly higher in comparison to location Arneberg. This highlights the importance of following the same protocol, but also to use the same equipment as far as it goes.

4.2.4 Correlation between UAV-images with spectral bands and VIs with DMY

The results from the correlation between vegetation indices calculated from reflectance values and yield indicates that the highest correlation for location Ås is 0.80 and is between red-edge and yield 24 days before first cut. For location Arneberg, 20 days before first cut (24.05.2022), the highest correlation is 0.70 between red-edge and yield. The correlations from the harvest day at Arneberg (13.06.2022) show a very low correlation and has a negative correlation with NDVI. High correlation between volume and plant height. For location one, the VIs related to NDVI correlate the most on the date (27-05-2022), in all hights, but the overall correlation seems to be higher at (25-05-2022). And last, a minimal difference in correlation between hights.

The correlations between image-data and yield from the trials at Arneberg include correlation with several vegetations indices (VI). Vegetation indices are mathematical combinations of wavelength-specific spectral reflectance, such as red, blue, green, red-edge and near-infrared (NIR). The VIs is developed to detect and monitor vegetation´s phenological conditions remotely (Barzin et al., 2020).

Vegetation by itself has a low reflectance of blue and red bands from the spectrum due to maximum chlorophyll absorption in those bands, while reflectance from the green bands has a peak. Because of a cellular structure in leaves, the reflectance is much more significant in NIR bands compared to visible bans such as red, green and blue (Barzin et al., 2020).

The included vegetations indices here are as mentioned in the results Excess Green (EXG), Meris Terrestrial Chlorophyll Index (MTCI), Excess Green minus Excess Red (EXGR), Green Normalized Difference Vegetation Index (GNDVI), Enhanced Vegetation Index (EVI), Simple Ratio (SR) as well as normalized Difference vegetation index (NDVI). Each are designed to measure a trait.

For the correlations from Ås, there is three heights to look and compare. 20 meters, 30 meters and 50 meters. With first glance it seems to be almost no different between the dates as well as the heights, but after a closer look, there is more correlation between other Vis and yield from 4 days after heading, first cut (25-05-2022), but NDVI correlate the most at 6 days after heading, first cut (27-05-2022). When looking at the height, the differences are minimal, but it is a slightly higher correlation at 50 meters. For example, plant height and volume for 20 meters has a 0.73 correlation, and for the same date at 50 meters, the correlation is 0.92. The NDVI correlation from 6 days after heading, first cut (27-05-2022) is for 15 meters 0.79 for fresh weight, and 0.80 for the same date and value from 50 meters. These findings contribute to the determination of height and date for yield prediction with a clear adventitious with a higher height and an earlier date for image capturing.

4.2.5 Correlation between UAV-images and yield from plots

The correlation between UAV-images and yield from the plots at location Arneberg yielded very poor results and made it impossible to compare rows and plots to each other as mentioned earlier. One reason for these poor results could be due to low quality UAV-images due to camera type or changes in imaging angle. This would make a huge impact on the image-quality and could definitely be a reason for poor results. This is a highly plausible reason, since the image data from Arneberg has been over all lower compared to Ås, despite the fact that Arneberg had a significantly higher yield. Since the number of flying heights was reduced at Arneberg, the only heights to inspect are 15 meters and 20 meters. This does not necessary mean that the data from the missing heights 30 meters and 50 meters would be better, since the data from 20 meters at rows from Ås was still significantly higher in comparison to location Arneberg. This highlights the importance of following the same protocol, but also to use the same equipment as far as it goes.

4.3 Regression analysis

4.3.1 Prediction of DMY compared to actual DMY, Location Ås

The results from the DMY prediction preformed on the yield and image data from location Ås indicate a good DMY prediction, specially from the first cut with multispectral images. The predictions made from RGB camera at Ås is lower than multispectral from the same location, but higher than the prediction from Arneberg. The prediction from the multispectral images at location one is similar for all heights, but the prediction is all over slightly better for 30 meters. For 10 days before the first cut which was 4 days after heading, first cut (25-05-2022) and the date of the first cut (02-06-2022) the results are the same despite which camera used. These findings contribute to the objectives to develop a protocol for UAV-phenotyping and to establish prediction and measurement model with the best height and date for DMY prediction. This type of prediction was previously proven with an R^2= 0.61-0.66 on plots with a size of 1.5m^2 and image-data captured at 20 meters above ground by Shorten & Trolove in 2022 (Shorten & Trolove, 2022). This correlation tells us that 61% of variance in DMY can be explained by a forage volume measured by UAV-imaging method. (Shorten & Trolove, 2022). In our own experiment, the same hight gave us a prediction with 91% of the variance in DMY explained by the forage volume measured by the UAV-images.

The prediction made from volume and plant height measured with RGB images from location Ås indicated a less precise prediction closer to the harvest.

4.3.2 Prediction of DMY compared to actual DMY, Location Arneberg

Prediction for the rows at Arneberg is made from multispectral UAV-images from 20 meters and the yield form the rows. The prediction for the plots is made from multispectral UAV-images captured at both 15 meters and 20 meters. Both rows and plots were also captured with RGB camera, but since these images was of so low quality due to a different angle than required for height and volume measurement, the results from these images were therefore not usable. Since the prediction from Arneberg lack both two of the heights (30m and 50m) and all images from RGB, the results cannot fully confirm a lower prediction for this specific location, it rather highlights the need to inspect all the different heights with both camera types. Based on the good results from Ås, there is of interest to inspect both the missing heights, as well as RGB properly.

The DMY prediction for the plots (table 15.) are using exclusively multispectral images due to the know error of the RGB images. The results in this table show that the prediction for both heights at the first cut are identical. Even though it's possible, it is a bit strange, and may indicate that there is something wrong with eighter of the data frames used in the prediction model. However, the prediction for the second cut is more expected. It is lower compared to rows from Arneberg, as well as results from location Ås, but the heights do give different results, and indicate a similar result as found in other parts of the results, which is that for multispectral imaging, the best results are obtained on a higher capturing height. The highest prediction was from multispectral images taken from 20 meters, five days before the second cut. While the prediction form 15 meters was higher at the earlier assessment date, the prediction was almost identical for 18 days before the second cut (0.43), and for five days before the second cut (0.44).

4.4 Develop of a protocol for UAV-phenotyping for yield predictions.

4.4.1 Our findings

The result from this study adds more points of view for developing a protocol for UAV-based phenotyping and yield prediction in ryegrass breeding. The findings from this study and the first season of the trial gave good results for the prediction with UAV-images, as well as details to remove and details to improve.

The predictions made from the image data from location Ås gave promising results for especially the first cut, with both multispectral and RGB camera. The reliability of the predictions is presented in 3.3.1, and pictures a high prediction specially for the first cut at Ås (table 12.) with an correlation coefficient above 0.90, which means that over 90% of variance in the DMY can be explained by the forage volume measured by the UAV-images.(Shorten & Trolove, 2022). For the second cut, the results were lower, but this was an all over observation for both camera-types and the four heights. This indicate that the data assessment for the first cut was successful, and the settings and assessment method worked. For future work, this should therefore be replicated to inspect if the outcome of the first and second cut will remain the same as the previously.

The results from location Arneberg did not give a lot of good results for yield prediction, but they highlighted several important issues for the protocol development. Since the image-data from this location was affected by methodological errors such as changes in the assessment schedule and

equipment settings. These results still gave the insight of how sensitive these methods are, and how important precision is in this type of experiment and development.

4.4.2 Future work

To fully develop a protocol for the ryegrass yield prediction with UAV-images, the results from this study should have had a more consistent outcome, which could promise more readability from the predictions preformed. This study does however not make all the necessary requirements for a fully developed protocol, but it gives important results for the future project and for the end goal of developing a protocol. Important factors to consider for protocol development is data precision and accuracy, reliability of predictions, ease of implementation, time required for data acquisition and processing. Results from this study has indicated that the number of flights preformed while imaging can be reduced due to the findings form the images captured in the 2022 season from location Ås. The results from the same location also gave findings that indicate that the flights can be reduced with both flight heights and flying's per week, as long as the goal is to capture phenological data for yield.

The first factor considered is data precision and accuracy, this part has been inspected with the correlation between the heights (3.2.1), table 4.) and the correlation with yield (3.2.3, 3.2.4 and 3.2.5). These results indicated a high correlation between the flights. For the multispectral camera, the best correlation was with a higher flight altitude such as 30 meters and 50 meters, while the RGB camera indicated a higher correlation at a lower altitude such as 15 meters and 20 meters. This knowledge correlate well with the results from 3.3.1 (Prediction of DMY compared to actual DMY), where the best predictions are from the higher heights at Ås with multispectral images (table 12.) and lower heights with RGB images (table 13.)

The factor ease of implementation is a simplified flight schedule and a premade workflow with each step simplified and explained. For this, based on our results I would recommend flights once a week, so it's possible to move the flight to a day with suitable weather, without missing out on a lot of image-data. This has also been proven possible since the flights every second day show little to no difference in values (table 4.). Since it's not easy to plan before the season when the harvests will occur, once a week is good interval when our results has shown a high prediction 10 days before the harvest, especially for multispectral (table 12.). The results from Arneberg gives a good example on the importance of a simplified flight schedule with the details of the assessment

being written and understandable. Since the flight mission is premade, and used for all flights at the specific trial, it is important that this is correct at the beginning.

Time required for both data collection and data processing is an important factor to include, since time often equals money. For data collection, the lower flights require more time since each image cover a smaller part of the trial. It also requires pauses for battery changes in the bigger trials. The higher flights however are much quicker since each picture capture much larger area of the whole trial and these flights was finished in under 10 minutes at Ås. The data processing is directly related to the collection since a lower flight needs to take more pictures than a higher flight. Therefore, the processing of the lower altitudes will take more time in the raw-image processing. This could mean several minutes or even hours for the largest fields (15 meters, multispectral images, plots). The smallest fields captured with 50 meters consisted of only 22 pictures for multispectral, and 3 pictures from RGB. So, for time consume, it would be advantageous to use the highest flight as possible.

4. Conclusion

The aims for this study are to develop a protocol for ryegrass phenotyping with UAV-imaging and determine the optimal flight altitude for ryegrass yield prediction and volume measurement. DMY prediction using spectral reflectance from five different spectral bands including red, green, blue, red edge and NIR. As well as to compare the RGB and multispectral imaging capabilities for DMY prediction. Our results in this study enabled the possibility to predict DMY with our correlation coefficient being 0.92 for the first cut. This was obtained with both multispectral images as well as RGB images. The maximum prediction was made with both multispectral images as well as RGB images. The flight altitude for multispectral images that yields best results are from 30 and 50 meters, while RGB images that yields best results are from 15 meters. The results from location Arneberg highlighted the importance of a detailed protocol, and how crucial it is to follow it while the experiment is in the development stage.

Our results have been found important for eliminating unnecessary flights, and to reduce the volume of data needing to be processed for the upcoming seasons. For furture studies, it is important to inspect the same heights that was found effective in the rows at location Ås on field sown in plots. For a protocol to be more accurate, it is important to gather successful data from more than one location and more than one season.

5. References

Alckmin, G. T., Lucieer, A., Rawnsley, R., & Kooistra, L. (2022). Perennial ryegrass biomass retrieval through multispectral UAV data. *Computers and Electronics in Agriculture*, *193*, 106574.

Ampatzidis, Y., & Partel, V. (2019). UAV-based high throughput phenotyping in citrus utilizing multispectral imaging and artificial intelligence. *Remote Sensing*, *11*(4), 410.

Araus, J. L., & Cairns, J. E. (2014). Field high-throughput phenotyping: the new crop breeding frontier. *Trends in plant science*, *19*(1), 52-61.

Barzin, R., Pathak, R., Lotfi, H., Varco, J., & Bora, G. C. (2020). Use of UAS multispectral imagery at different physiological stages for yield prediction and input resource optimization in corn. *Remote Sensing*, *12*(15), 2392.

Bhandari, M., Chang, A., Jung, J., Ibrahim, A. M., Rudd, J. C., Baker, S., Landivar, J., Liu, S., & Landivar, J. (2023). Unmanned aerial system‐based high‐throughput phenotyping for plant breeding. *The Plant Phenome Journal*, *6*(1), e20058.

Borra‐Serrano, I., De Swaef, T., Muylle, H., Nuyttens, D., Vangeyte, J., Mertens, K., Saeys, W., Somers, B., Roldán‐Ruiz, I., & Lootens, P. (2019). Canopy height measurements and non‐destructive biomass estimation of Lolium perenne swards using UAV imagery. *Grass and Forage Science*, *74*(3), 356-369.

Brereton, A., & McGilloway, D. (1999). Winter growth of varieties of perennial ryegrass (Lolium perenne L.). *Irish Journal of Agricultural and Food Research*, 1-12.

Burud, I., Lange, G., Lillemo, M., Bleken, E., Grimstad, L., & From, P. J. (2017). Exploring robots and UAVs as phenotyping tools in plant breeding. *IFAC-PapersOnLine*, *50*(1), 11479-11484.

Cedric, L. S., Adoni, W. Y. H., Aworka, R., Zoueu, J. T., Mutombo, F. K., Krichen, M., & Kimpolo, C. L. M. (2022). Crops yield prediction based on machine learning models: case of west african countries. *Smart Agricultural Technology*, 100049.

Cunningham, P. J., Blumenthal, M. J., Anderson, M. W., Prakash, K. S., & Leonforte, A. (1994). Perennial Ryegrass Improvement in Australia. *New Zealand Journal of Agricultural Research*, *37*(3), 295-310. https://doi.org/Doi 10.1080/00288233.1994.9513068

Dash, J., & Curran, P. (2007). Evaluation of the MERIS terrestrial chlorophyll index (MTCI). *Advances in Space Research*, *39*(1), 100-104.

Dobbels, A. A., & Lorenz, A. J. (2019). Soybean iron deficiency chlorosis high-throughput phenotyping using an unmanned aircraft system. *Plant methods*, *15*(1), 1-9.

Fakta om Landbruk. (2023). Statistisk Sentralbyrå. https://www.ssb.no/jord-skog-jakt-og-fiskeri/faktaside/jordbruk

Fan, X., Kawamura, K., Xuan, T. D., Yuba, N., Lim, J., Yoshitoshi, R., Minh, T. N., Kurokawa, Y., & Obitsu, T. (2018). Low-cost visible and near-infrared camera on an unmanned aerial vehicle for assessing the herbage biomass and leaf area index in an Italian ryegrass field. *Grassland science*, *64*(2), 145-150. https://doi.org/https://doi.org/10.1111/grs.12184

Frame, J. (1989). Herbage productivity of a range of grass species under a silage cutting regime with high fertilizer nitrogen application. *Grass and Forage Science*, *44*(3), 267-276.

Gebremedhin, A., Badenhorst, P., Wang, J., Giri, K., Spangenberg, G., & Smith, K. (2019). Development and validation of a model to combine NDVI and plant height for high-throughput phenotyping of herbage yield in a perennial ryegrass breeding program. *Remote Sensing*, *11*(21), 2494.

Gebremedhin, A., Badenhorst, P., Wang, J., Shi, F., Breen, E., Giri, K., Spangenberg, G. C., & Smith, K. (2020). Development and validation of a phenotyping computational workflow to predict the biomass yield of a large perennial ryegrass breeding field trial. *Frontiers in Plant Science*, *11*, 689.

Gebremedhin, A., Badenhorst, P. E., Wang, J., Spangenberg, G. C., & Smith, K. F. (2019). Prospects for measurement of dry matter yield in forage breeding programs using sensor technologies. *Agronomy*, *9*(2), 65.

Ghamkhar, K., Irie, K., Hagedorn, M., Hsiao, J., Fourie, J., Gebbie, S., Hoyos-Villegas, V., George, R., Stewart, A., & Inch, C. (2019). Real-time, non-destructive and in-field foliage yield and growth rate measurement in perennial ryegrass (Lolium perenne L.). *Plant methods*, *15*(1), 1-12.

Hannaway, D., Fransen, S., Cropper, J. B., Teel, M., Chaney, M., Griggs, T., Halse, R. R., Hart, J. M., Cheeke, P. R., & Hansen, D. E. (1999). Perennial ryegrass (Lolium perenne L.).

Jung, G., Van Wijk, A., Hunt, W., & Watson, C. (1996). Ryegrasses. *Cool‐season forage grasses*, *34*, 605-641.

Jypiter Notebook. https://jupyter.org

Khan, Z., Rahimi-Eichi, V., Haefele, S., Garnett, T., & Miklavcic, S. J. (2018). Estimation of vegetation indices for high-throughput phenotyping of wheat using aerial imaging. *Plant methods*, *14*(1), 1-11.

Kim, I.-H., Jeon, H., Baek, S.-C., Hong, W.-H., & Jung, H.-J. (2018). Application of crack identification techniques for an aging concrete bridge inspection using an unmanned aerial vehicle. *Sensors*, *18*(6), 1881.

Leddin, C., Jacobs, J., Smith, K., Giri, K., Malcolm, B., & Ho, C. (2018). Development of a system to rank perennial ryegrass cultivars according to their economic value to dairy farm businesses in south-eastern Australia. *Animal Production Science*, *58*(8), 1552-1558.

Liu, H., Qi, Y., Xiao, W., Tian, H., Zhao, D., Zhang, K., Xiao, J., Lu, X., Lan, Y., & Zhang, Y. (2022). Identification of Male and Female Parents for Hybrid Rice Seed Production Using UAV-Based Multispectral Imagery. *Agriculture*, *12*(7), 1005.

Lootens, P., Ruttink, T., Rohde, A., Combes, D., Barre, P., & Roldán-Ruiz, I. (2016). High-throughput phenotyping of lateral expansion and regrowth of spaced Lolium perenne plants using on-field image analysis. *Plant methods*, *12*(1), 1-14.

Ludovisi, R., Tauro, F., Salvati, R., Khoury, S., Mugnozza Scarascia, G., & Harfouche, A. (2017). UAV-based thermal imaging for high-throughput field phenotyping of black poplar response to drought. *Frontiers in Plant Science*, *8*, 1681.

Lunnan, T. E., Martha. (2011, 28.02.2022). *Høstetidspunkt i eng*. Agropub. Retrieved 26.06.2023 from https://www.agropub.no/fagartikler/haustetidspunkt-i-eng

Marum, P. (2016). Norsk raigras er god økonomi. *Norsk Landbruk*, *nr 6.*

Meyer, G. E., & Neto, J. C. (2008). Verification of color vegetation indices for automated crop imaging applications. *Computers and Electronics in Agriculture*, *63*(2), 282-293.

Moeinizade, S., Pham, H., Han, Y., Dobbels, A., & Hu, G. (2022). An applied deep learning approach for estimating soybean relative maturity from UAV imagery to aid plant breeding decisions. *Machine Learning with Applications*, *7*, 100233.

NIBIO. (2023). *Gårdskart* https://gardskart.nibio.no/search

Pranga, J., Borra-Serrano, I., Aper, J., De Swaef, T., Ghesquiere, A., Quataert, P., Roldán-Ruiz, I., Janssens, I. A., Ruysschaert, G., & Lootens, P. (2021). Improving accuracy of herbage yield predictions in perennial ryegrass with uav-based structural and spectral data fusion and machine learning. *Remote Sensing*, *13*(17), 3459.

Rallo, P., de Castro, A. I., López-Granados, F., Morales-Sillero, A., Torres-Sánchez, J., Jiménez, M. R., Jiménez-Brenes, F. M., Casanova, L., & Suárez, M. P. (2020). Exploring UAV-imagery to support genotype selection in olive breeding programs. *Scientia Horticulturae*, *273*, 109615.

Repstad, J. A. (2023). *Valg av såfrø til eng*. https://www.felleskjopet.no/alle-artikler/alle-artikler-planteproduksjon/artikler/valg-av-safro-til-eng/

Reynolds, M., Chapman, S., Crespo-Herrera, L., Molero, G., Mondal, S., Pequeno, D. N., Pinto, F., Pinera-Chavez, F. J., Poland, J., & Rivera-Amado, C. (2020). Breeder friendly phenotyping. *Plant Science*, *295*, 110396.

Shorten, P., & Trolove, M. (2022). UAV-based prediction of ryegrass dry matter yield. *International Journal of Remote Sensing*, 1-17.

Song, P., Wang, J., Guo, X., Yang, W., & Zhao, C. (2021). High-throughput phenotyping: Breaking through the bottleneck in future crop breeding. *The Crop Journal*, *9*(3), 633-645.

Steinshamn, H., Nesheim, L., & Bakken, A. (2016). Grassland production in Norway. *Grassland Science in Europe*, *21*, 4-8.

Wang, J., Badenhorst, P., Phelan, A., Pembleton, L., Shi, F., Cogan, N., Spangenberg, G., & Smith, K. (2019). Using sensors and unmanned aircraft systems for high-throughput phenotyping of biomass in perennial ryegrass breeding trials. *Frontiers in Plant Science*, *10*, 1381.

Wilkins, P., & Humphreys, M. (2003). Progress in breeding perennial forage grasses for temperate agriculture. *The Journal of Agricultural Science*, *140*(2), 129-150.

Xie, C., & Yang, C. (2020). A review on plant high-throughput phenotyping traits using UAV-based sensors. *Computers and Electronics in Agriculture*, *178*, 105731.

Yates, S., Jaškūnė, K., Liebisch, F., Nagelmüller, S., Kirchgessner, N., Kölliker, R., Walter, A., Brazauskas, G., & Studer, B. (2019). Phenotyping a Dynamic Trait: Leaf Growth of Perennial Ryegrass Under Water Limiting Conditions [Original Research]. *Frontiers in Plant Science*, *10*. https://doi.org/10.3389/fpls.2019.00344

6. Appendix

Appendix 1. Figures

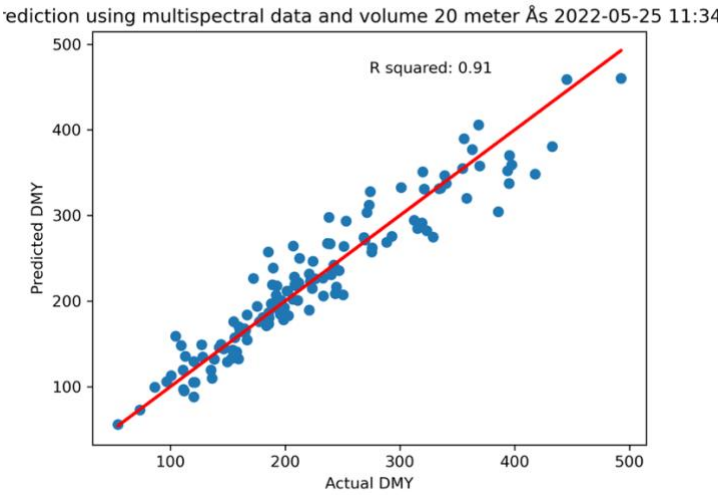

Figure 14. Prediction from multispectral images captured at 20 meters. first cut Ås

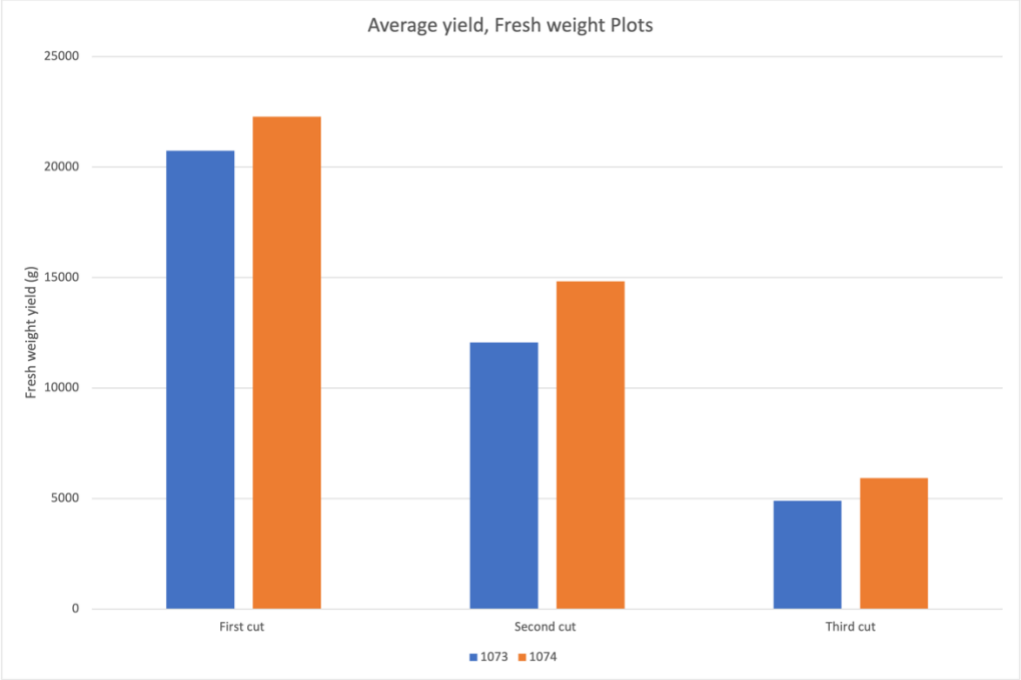

Figure 15. Average fresh weight yield from plots at Arneberg

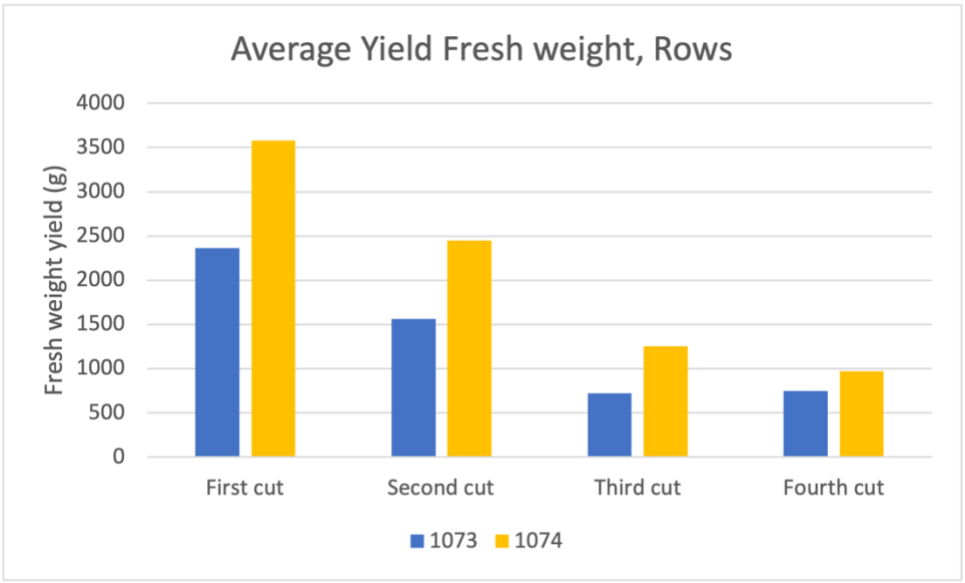

Figure 16. Bar plot of the yield from location two (Graminor), row trials. 1073 as blue and 1074 as yellow.

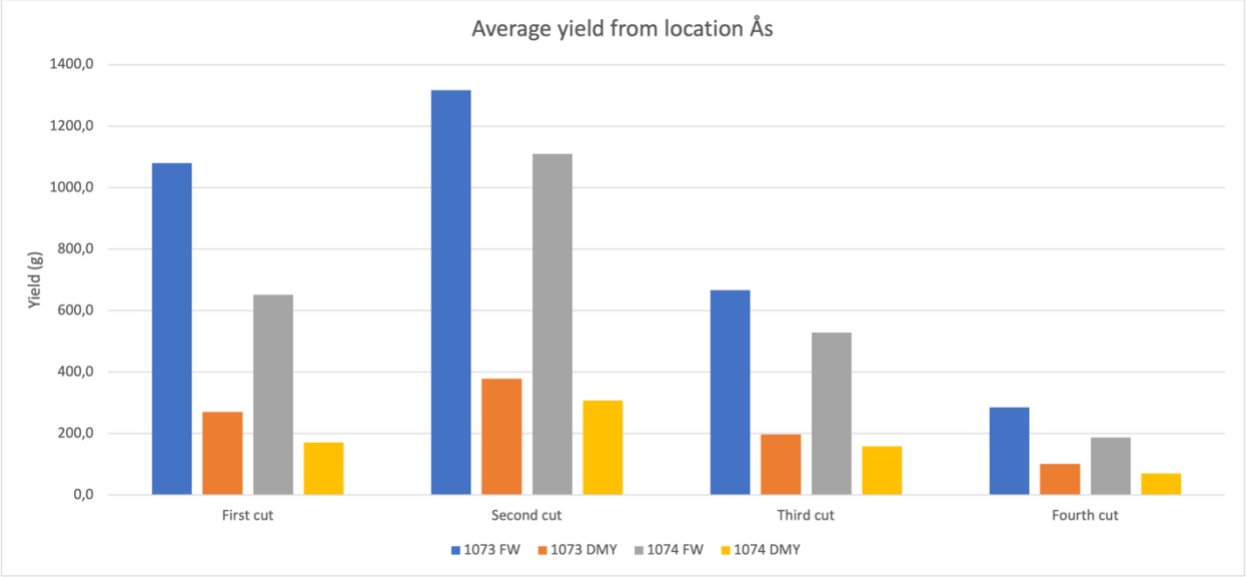

Figure 17. Bar plot of yield from Ås, each colour shows a different calculated value of yield. Blue = Diploid fresh weight, orange = Diploid dry matter yield, grey = Tetraploid fresh weights, and yellow = Tetraploid dry matter yield.

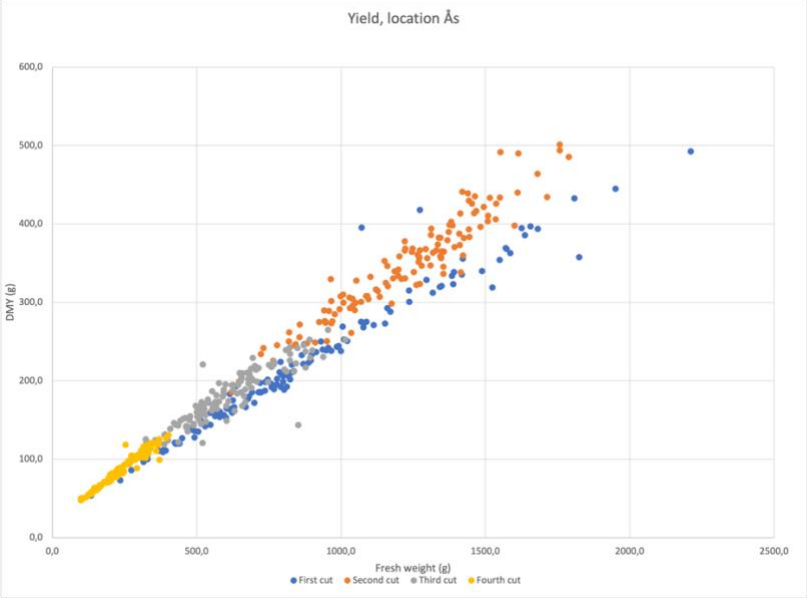

Figure 18. Scatterplot of relationship between fresh weight and dry matter yield at Ås. Blue = yield from first cut, Orange = yield from second cut, grey = yield from third cut, and yellow = yield from fourth cut.

Appendix 2. Tables

Table 16. Comparison of yield between tetraploid rows and plots at Arneberg, first and second cut. Fresh yield in gram

First cut			Second cut		
	Rows	Plots		Rows	Plots
Raite	3753,3	20607,3	Fagerlin	2585,3	12352,3
Fagerlin	3514	20793,6	Fagerlin+Trygve	2850	13336,3
PG-4x	3181,3	21055,6	Fagerlin+Birger	2282,6	13496,6
Figgjo+Trygve+Birger	3132	21146	Fagerlin+Raminta	2478	13692,6
Fagerlin+Trygve	3568	21493,6	Fagerlin+Figgjo+Trygve	2898,6	13813,3
Fagerlin+Raite	3439,3	21835,6	Fagerlin+Figgjo+Trygve+Birger	2302,6	13935,3
PM-4x	3979,3	22136	PM-4x	2432	14231,3
Trygve	3758,6	22139	Trygve	2051,3	14237
Fagerlin+Raminta	3379,3	22172	Fagerlin+Raite	2792,6	14542
Fagerlin+Figgjo+Trygve+Birger	3711,3	22199,6	Figgjo+Trygve+Birger	2424,6	14646,6
GnRa1576-4x	3568	22425,3	EST-WP3-4x	2266	14768,6
PN-4x	3722,6	22514	Birger	2494	14829
Fagerlin+Figgjo+Trygve	3595,3	22628,6	GnRa1576-4x	2242	15427,6
EST-WP3-4x	3714	22977,3	Fagerlin+Figgjo+Birger	3148	15472
Figgjo	3726,6	23082,3	PG-4x	2466	15545,6
Fagerlin+Figgjo+Birger	3842	23136,6	PN-4x	2688,6	16030,6

Birger	3746	23224,	Raite	2535,3	16120,3
Fagerlin+Birger	3155,3	23285,6	Figgjo	2223,3	16169
Raminta	3527,3	23296,6	Fagerlin+Figgjo	2533,3	16328,3
Fagerlin+Figgjo	3510,6	23400	Raminta	1636	17282,3

Table 17. Comparison of yield between rows and plots in diploid trial at Arneberg, first and second cut.

First cut	Column1	Column2	Second cut	Column1	Column2
	Rows	Plots		Rows	Plots
17-SV1-17607/1	2380,6	18238,3	EST-WP3-2x	1678,6	9696,6
PG-2X	2540,6	19406,6	Raidi	1524	10421
17-SV1-17608/1	2224	19655	PB-2x	1358	10807
PK-2x	2305,3	19804,6	17-SV1-17607/1	1474	10973
PE-2x	2240	19839,6	PF-2x	1750,6	11053,3
PB-2x	2268,6	20134	PE-2x	1537,3	11095,3
GnRa1575-2x	2599,3	20212,6	PK-2x	1846,6	11156,6
PI-2x	2410,6	20256	PL-2x	1391,3	11207
PC-2x	2592,6	20335,6	PA-2x	1636	11564,6

17-SV1-17503/1	2326,6	20494	FuRa9601-2x	1520,6	11603,3
PD-2x	2094,6	20529	PD-2x	1662	11930,6
PL-2x	2492,6	20609,3	17-SV1-17606/1	1852	12094,3
17-SV1-17606/1	2635,3	20709,6	17-SV1-17605/1	1363,3	12182,3
17-SV1-17602/1	2585,3	21201,3	PC-2x	1548	12421,3
PA-2x	2246	21495,3	17-SV1-17602/1	1784	12673,6
EST-WP3-2x	2308,6	21344,6	17-SV1-17604/1	1604	12734
Raidi	2311,3	21463,3	17-SV1-17608/1	1444	13004,6
PF-2x	2362,6	21610,6	GnRa1575-2x	1462,6	13074,3
PH-2x	2466,6	21645,6	PI-2x	1448	13086,6
17-SV1-17601/1	2137,3	21719,6	17-SV1-17503/1	1174	13152,3
FuRa9601-2x	2048,6	22024,6	17-SV1-17601/1	1513,3	13352
17-SV1-17605/1	2378,6	22228	PH-2x	1732,6	13705,3

17-SV1-17604/1	2407,3	22254	PG-2X	1570,6	14472,6

Table 18. Average yield for each trial and cut for location Ås. (g)				
Column1	First cut	Second cut	Third cut	Fourth cut
1073 FW	1079,4	1316,9	666,6	285,8
1073 DMY	270,3	378,7	196,9	101,7
1074 FW	651,9	1110,0	528,0	186,8
1074 DMY	170,9	307,7	159,2	70,8

Table 19. Registration stages throughout the season, with recorded dates.

	Growth start	Heading first cut	Heading second cut	Heading third cut
Ås	01.05.2022	21.05.2022	23.06.2022	02.08.2022
Arneberg	12.05.2022	04.06.2022-15.06.2022		

Table 20. Stages of development in grasses. Scale from Inst. for norrländsk växtodling Röbäcksdalen (modified) (Lunnan, 2011)

Stage of development	1. Leaf	2. Stem shooting	3. Beginning shooting	4. Shooting	5. Full Shooting
Explanation	Leaf and elongated leaf sheath.	At least one culm node on minimum 50% of the stem.	Some part of the spikelet is visible on at least 10 % of the shoots	Half of the spikelet is over the flag leaf on at least 50% of the shoots.	A part of the stem supporting the spikelet (peduncle) is visible on at least 50% of the shoots.

Table 21. Average fresh yield from diploid rows at location Ås			
Average Diploid			
First cut		Secodn cut	
PG-2x	610,0	PG-2x	1499,3
PB-2x	621,6	PB-2x	1028,4
PD-2x	636,0	PD-2x	1472,3
17-SV1-17602/1	663,8	17-SV1-17602/1	1052,3
17-SV1-17607/1	723,4	17-SV1-17607/1	1007,7
17-SV1-17608/1	734,1	17-SV1-17608/1	1286,3
PC-2x	812,6	PC-2x	899,2
PL-2x	844,0	PL-2x	1133,9
17-SV1-17503/1	884,9	17-SV1-17503/1	1202,3
17-SV1-17606/1	1016,1	17-SV1-17606/1	1467,1
PF-2x	1097,6	PF-2x	1418,0
17-SV1-17604/1	1125,3	17-SV1-17604/1	1166,3
PI-2x	1135,1	PI-2x	1224,3
PK-2x	1138,8	PK-2x	1328,7
PH-2x	1224,3	PH-2x	1661,9
PE-2x	1232,6	PE-2x	1497,7
17-SV1-17601/1	1246,5	17-SV1-17601/1	1423,1

Fagerlin	1299,7	Fagerlin	1338,7
17-SV1-17605/1	1335,9	17-SV1-17605/1	1430,1
EST-WP3-2x	1380,0	EST-WP3-2x	1368,8
PA-2x	1447,7	PA-2x	1418,8
GnRa1575-2x	1705,3	GnRa1575-2x	1320,2
Raidi	1910,8	Raidi	1568,7

Table 22. Average fresh yield from tetraploid rows at location Ås

Average Tetraploid			
First cut		Second cut	
Trygve	374,8	Trygve	1028,8
EST-WP3-4x	407,4	EST-WP3-4x	894,1
PM-4x	434,3	PM-4x	870,0
Pg-4x	473,8	Pg-4x	1259,9
PN-4x	506,8	PN-4x	1179,3
Raminta	509,1	Raminta	1144,0
Fagerlin+Figgjo	525,0	Fagerlin+Figgjo	876,7
Figgjo	584,4	Figgjo	1084,4
Fagerlin+Figgjo+Trygve	608,7	Fagerlin+Figgjo+Trygve	1070,7
Fagerlin+Raminta	633,2	Fagerlin+Raminta	1089,7
Fagerlin+Trygve	650,7	Fagerlin+Trygve	1087,3
Fagerlin	653,0	Fagerlin	966,5
Fager+Figg+Tryg+Birger	674,8	Fager+Figg+Tryg+Birger	1052,4
Figgjo+Trygve+Birger	699,6	Figgjo+Trygve+Birger	1229,1
Fagerlin+Figgjo+Birger	719,5	Fagerlin+Figgjo+Birger	1118,7
GnRa1576-4x	720,1	GnRa1576-4x	1140,9
Raite	761,8	Raite	1355,8
Fagerlin+Birger	909,9	Fagerlin+Birger	1181,2
Fagerlin+Raite	961,2	Fagerlin+Raite	1261,1
Birger	1030,0	Birger	1310,1

Appendix 3. Pictures from the field and the equipment

Figure 19. The haldrup harvester used at location Ås.

Figure 20. Overview of the row trial at location Arneberg at harvest, taken with UAV.

Norges miljø- og biovitenskapelige universitet
Noregs miljø- og biovitskapelege universitet
Norwegian University of Life Sciences

Postboks 5003
NO-1432 Ås
Norway